Positron annihilation in flight: experiment with slow and fast positrons

J. Čížek, M. Vlček, F. Lukáč, O. Melikhova, I. Procházka

Faculty of Mathematics and Physics, Charles University Prague, Czech Republic

W. Anwand, A. Wagner, M. Butterling

Institut für Strahlenphysik, Helmholtz-Zentrum Dresden-Rossendorf, Germany

R. Krause-Rehberg

Martin-Luther University, Halle, Germany

Introduction

- positrons in solid matter are thermalized within a few ps
- thermalized positron $\rightarrow$ annihilation in rest

  dominating process in solids
- non-thermalized positron $\rightarrow$ annihilation in flight (AiF)

  rare process (~ 1% fraction of positrons)

Annihilation in flight

- single quantum annihilation in flight (SQAF)

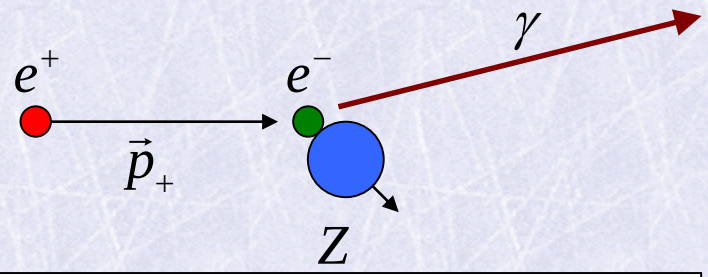

- cross-section (Bhabha 1934)

$$\sigma_{SQAF} = \frac{4\pi\alpha^4 Z^5 r_0^2}{\sqrt{T_+\left(T_+ + 2m_0c^2\right)^5}}\left[T_+\left(T_+ + \frac{8}{3}m_0c^2\right) + 3m_0c^2 - \frac{T_+ + 3m_0c^2}{\sqrt{T_+\left(T_+ + 2m_0c^2\right)}}\ln\left(T_+ + m_0c^2 + \sqrt{T_+\left(T_+ + 2m_0c^2\right)}\right)\right]$$

H.J. Bhabha, H.R. Hulme, Proc. Roy. Soc. (London) A146, 723 (1934)

- T_+ - positron kinetic energy, r_0 – classical electron radius, m_0c^2 – rest energy of electron
  Z_+ - atomic numer of target, α – fine structure constant

- important only in high-Z materials and for high positron energies

Annihilation in flight

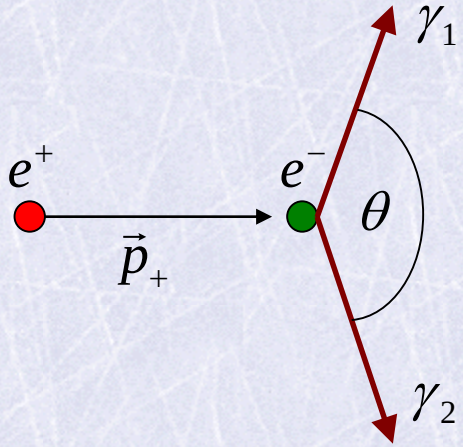

- two quantum annihilation in flight (TQAF)
- cross-section (Dirac 1934)

$$\sigma_{TQAF} = \pi r_0^2 \frac{1}{\gamma+1}\left[\frac{\gamma^2+4\gamma+1}{\gamma^2-1}\ln\left(\gamma+\sqrt{\gamma^2-1}\right)-\frac{\gamma+3}{\sqrt{\gamma^2-1}}\right]$$

P. A. M. Dirac, Proc. Camb. Phil. Soc. 26, 361 (1930)

- $\gamma = (T_+ + m_0c^2) / m_0c^2$, r_0 – classical electron radius, m_0c^2 – rest energy of electron, T_+ - positron kinetic energy

- main AiF channel

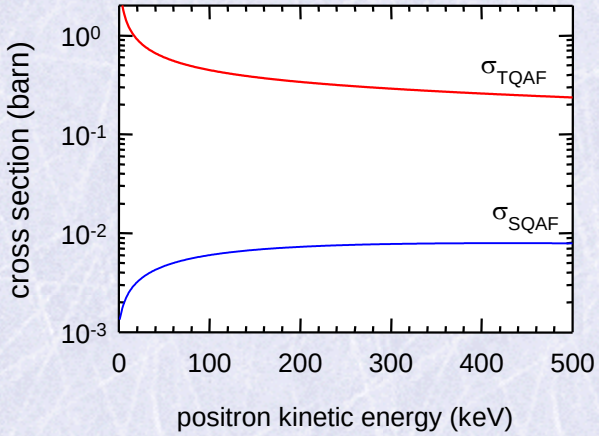

Investigations of annihilation in flight

- **early measurements:**

  - monoenergetic positrons 1-200 MeV
  - beta and gamma scintillation counters
  - good agreement with QED theoretical prediction

    S. A. Colgate and F.C. Gilbert, Phys. Rev. 89, 790 (1953)

    H. W. Kendall and M. Deutsch, Phys. Rev. 101, 20 (1956)

- **searching for resonances** near $W^{\pm}$ and Z^0 mass and signatures of new particles

  S.H. Connell et al., Phys. Rev. Lett. 60, 2242 (1988)

  E. Fernandez et al., Phys. Rev. D 35, 1 (1987)

  M.Z. Akrawy et al., Phys. Lett. B 257, 531 (1991)

CDB investigations of annihilation in flight

- **coincidence Doppler broadening spectroscopy (CDB)**

- precise coincidence measurement of energies of both annihilation quanta

- suitable tool for energy-resolved investigation of TQAF

- M. Weber and A.W. Hunt (1999)

- CDB studies of TQAF using mono energetic positron beam (T_+ = 10-72 keV)

- thin target

M. Weber et al., Phys. Rev. Lett. 83, 4658 (1999)

A. W. Hunt et al., Appl. Surf. Sci. 149, 282 (1999)

- F. Bečvář (2002) CDB observation of TQAF using fast positron emitted by ^{22}Na

F. Bečvář, talk at the workshop EPOS02 (2002) ($T_{+,max}$ = 545 keV)

- J. Dryzek (2007) CDB study of TQAF using fast positron emitted by ^{68}Ge/^{68}Ga

J. Dryzek et al., Radiation Physics and Chemistry 76, 297 (2007) ($T_{+,max}$ = 1897 keV)

Digital CDB spectrometer

digital CDB spectroscopy

- pulses from HPGe detetors are sampled by 12-bit digitizer (sampling period 20 ns)
- sampled waveforms are analyzed off-line by software

  J. Čížek et al., Nucl. Instrum. Methods A 623, 982 (2010)

  J. Čížek et al., New. J. Phys. 14, 035005 (2012)
- semi-digital configuration:

  - detector pulses are sharpened in spectroscopy amplifier prior to sampling

  - improvement of signal-to-noise ratio (s/n)

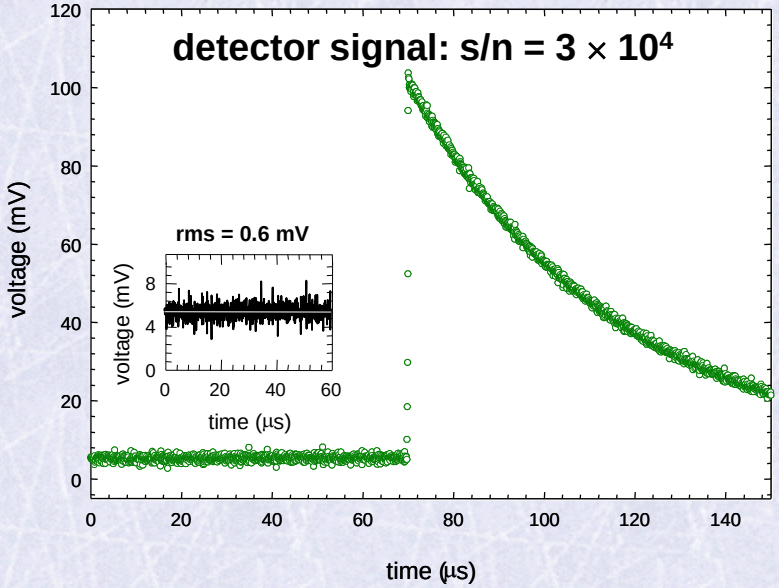

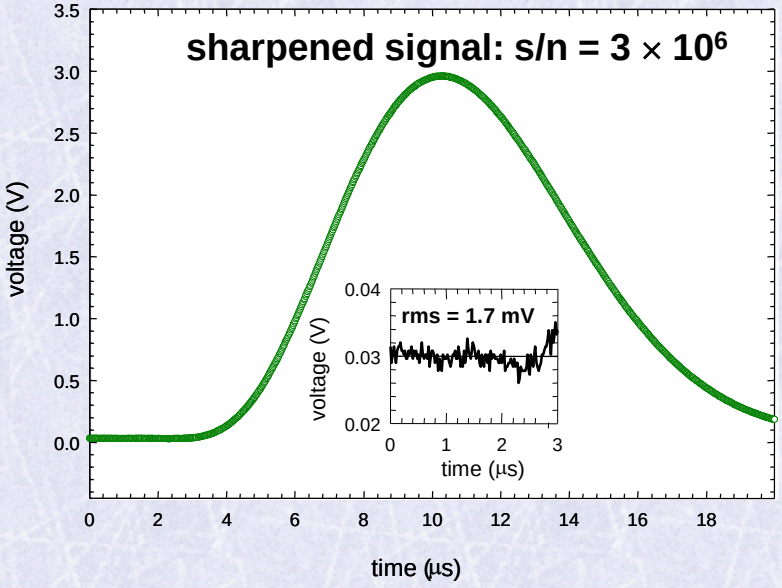

Digital CDB spectrometer: semi-digital setup

J. Čížek et al., Nucl. Instrum. Methods A 623, 982 (2010)

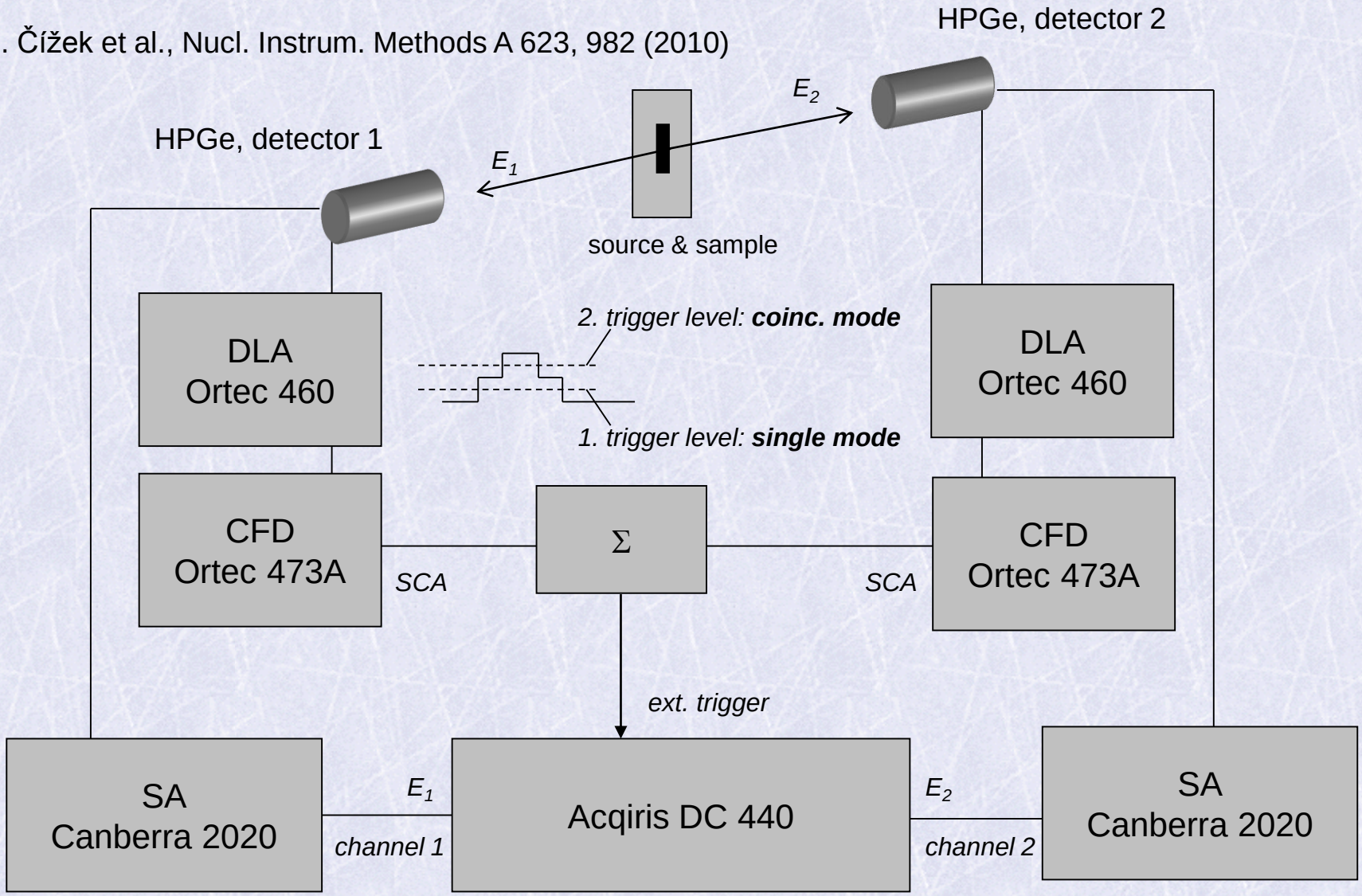

1 waveform = 1000 points
sampling rate = 50 MHz (sampling interval = 20 ns)

Digital CDB spectroscopy - analysis of data

run 1

read waveform

find maximum

calculate derivative

calculate background

apply “fixed” filters

failed

passed

calculate height

normalize & shift

add height to histogram

add pulse to histogram

calibrate energy spectrum

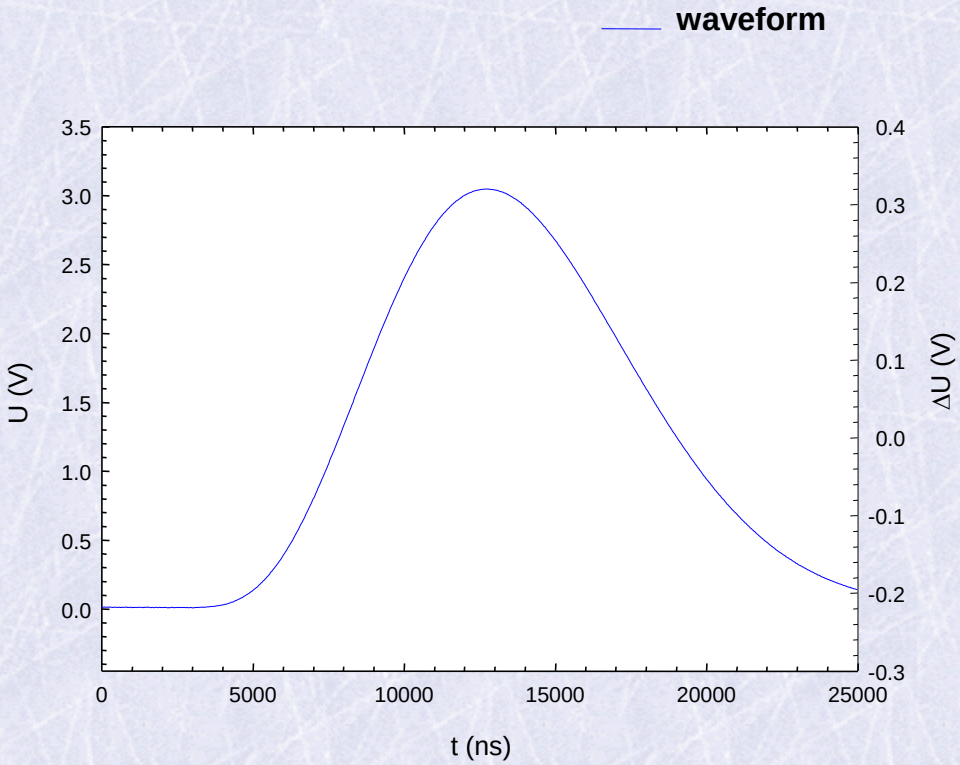

Digital CDB spectroscopy - analysis of data

run 1

read waveform

find maximum

calculate derivative

calculate background

apply “fixed” filters

failed

passed

calculate height

normalize & shift

add height to histogram

add pulse to histogram

calibrate energy spectrum

parabolic fitting

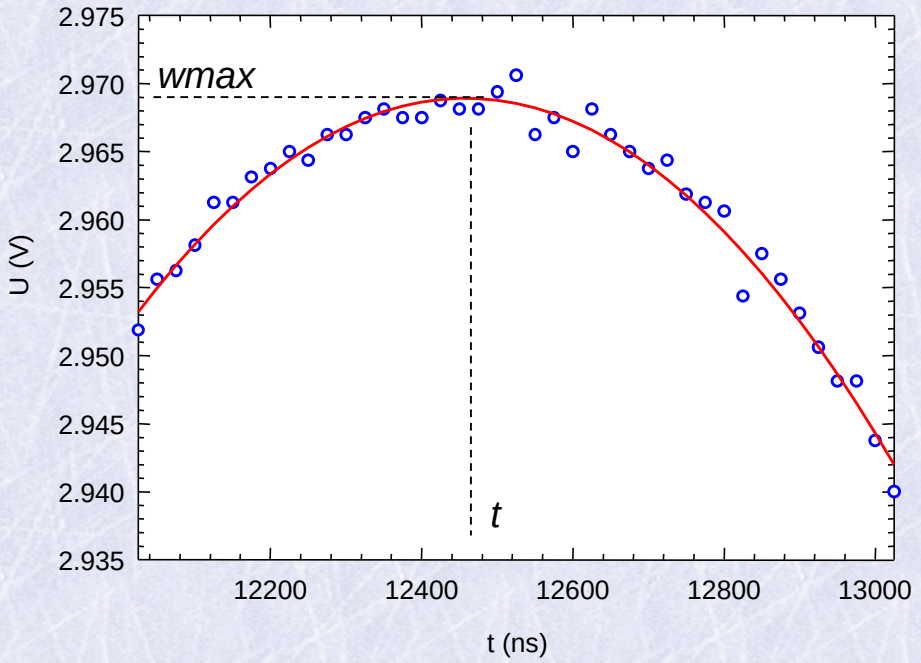

Digital CDB spectroscopy - analysis of data

run 1

read waveform

find maximum

calculate derivative

calculate background

apply “fixed” filters

failed

passed

calculate height

normalize & shift

w_{max}-baseline

add height to histogram

add pulse to histogram

calibrate energy spectrum

parabolic fitting

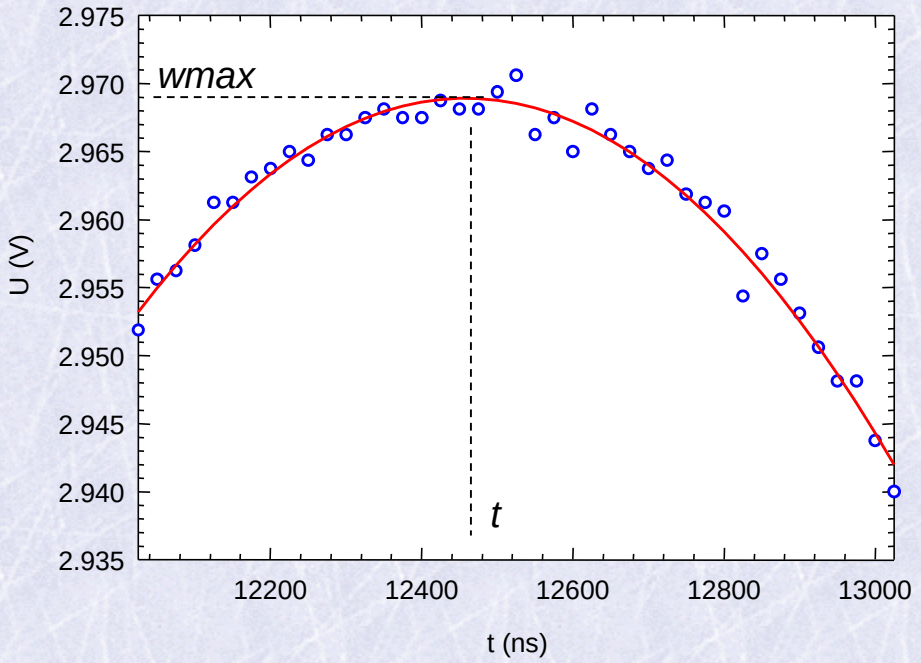

Digital CDB spectroscopy – shape filters

Two-dimensional histogram of normalized waveforms

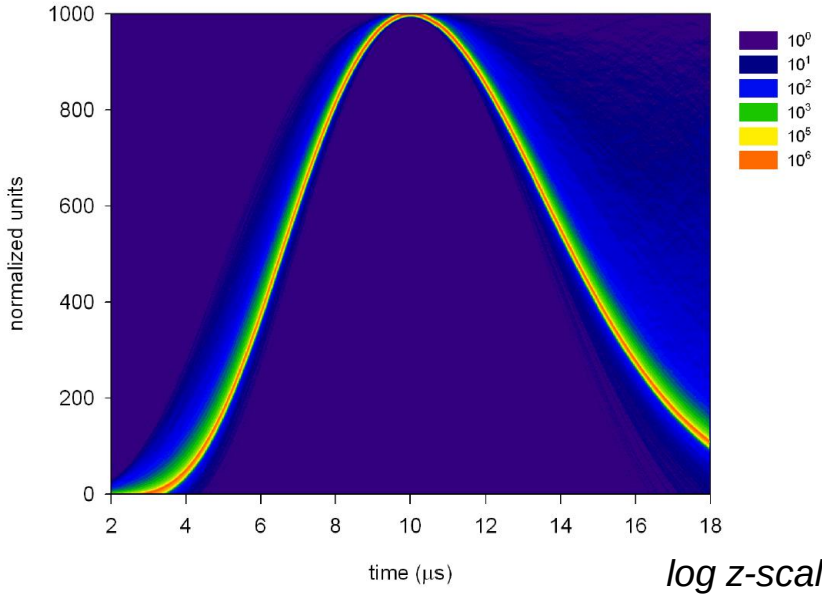

log z-scale

vertical cut of 2D pulse shape histogram

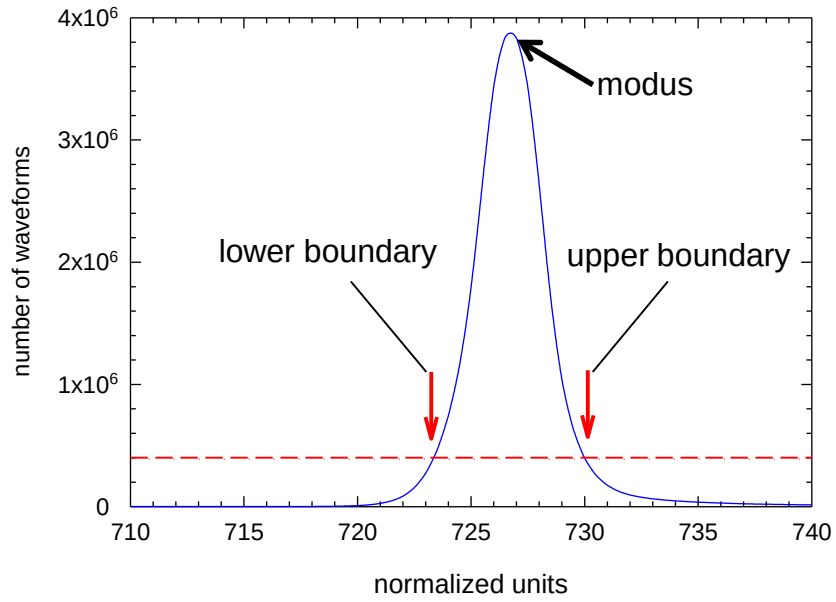

Digital CDB spectroscopy – shape filters

Two-dimensional histogram of normalized waveforms

all pulses

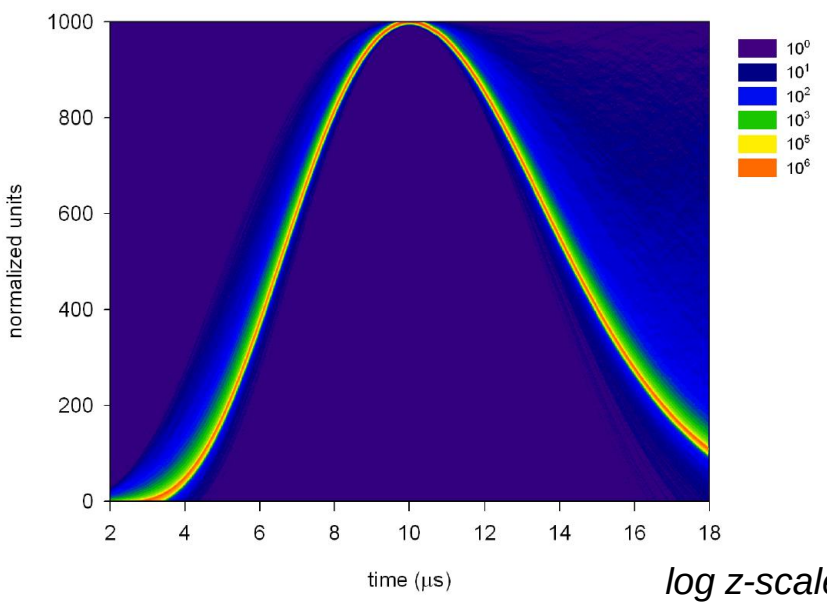

log z-scale

pulses accepted by shape filter

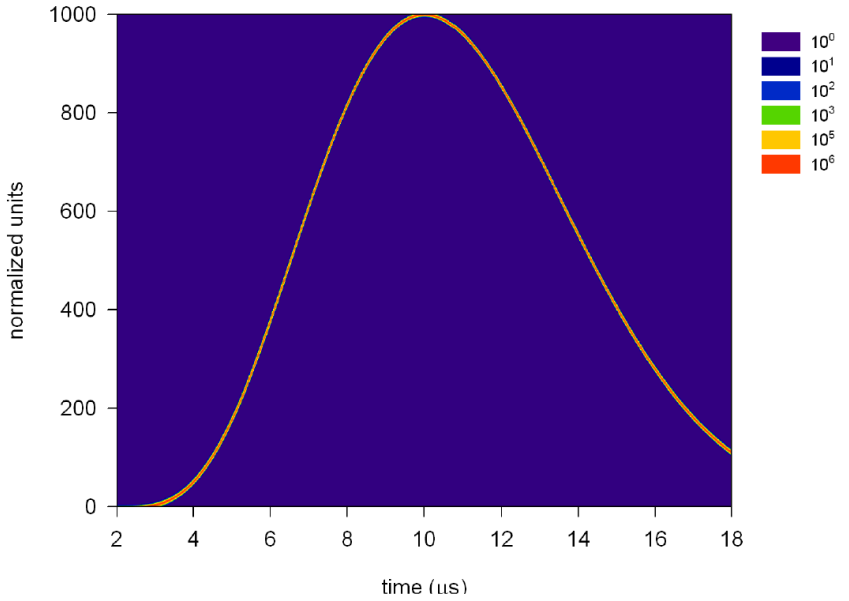

Digital CDB spectroscopy – CDB spectra

Two-dimensional CDB spectrum

sum of energies of annihilation gamma rays plotted versus difference of these energies

$E_1 + E_2 - 2m_0c^2$ versus $E_1 - E_2$

- pure Al (99.9999%)

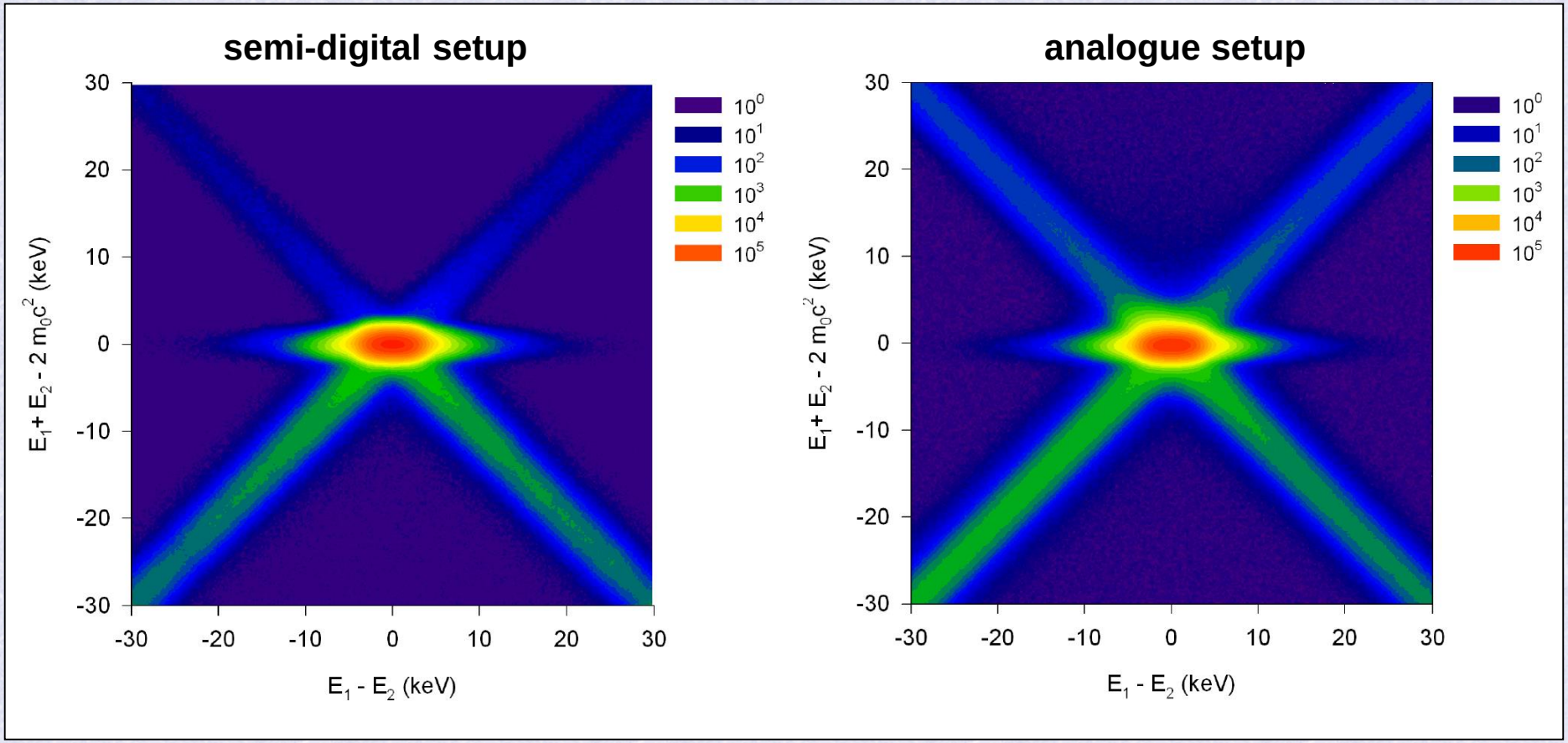

Digital CDB spectroscopy – CDB spectra

Two-dimensional CDB spectrum – effect of shape filters

- semi-digital setup
- pure Al (99.9999%)

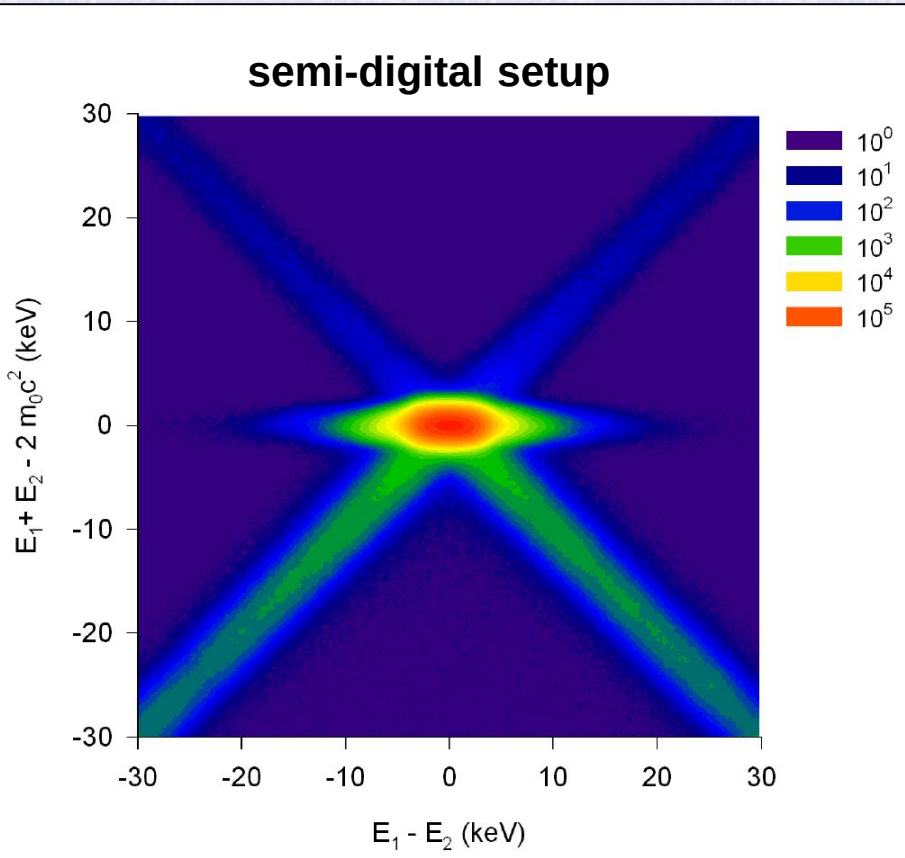

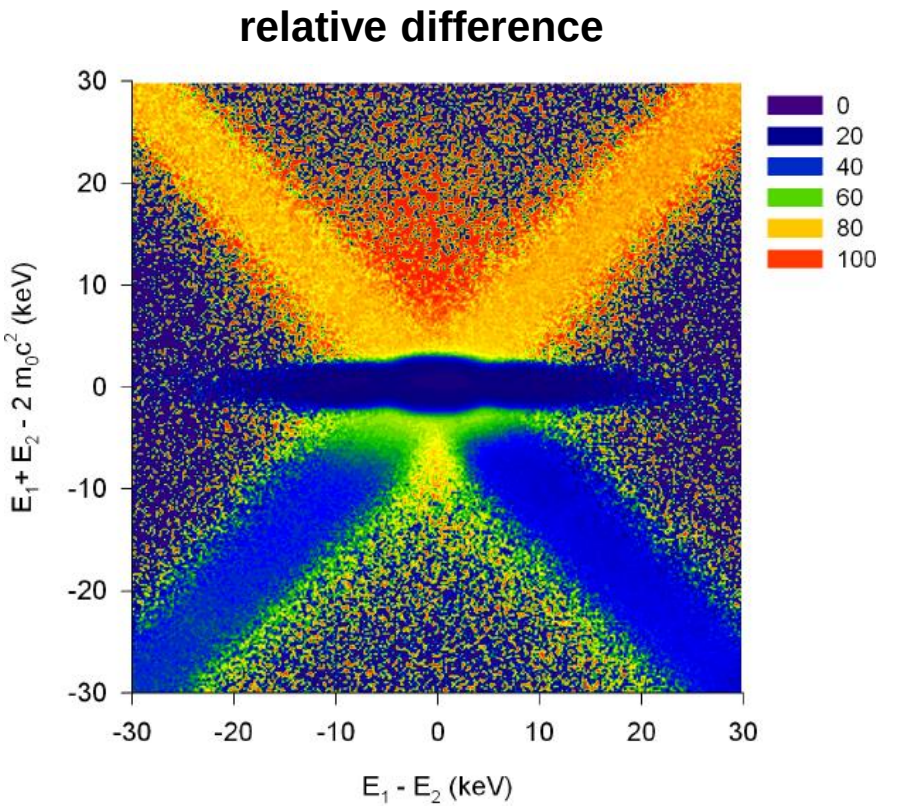

TQAF investigations – positron sources

- **monoenergetic slow positrons**

  - magnetically guided slow positron beam, SPONSOR

  - Helmholtz Zentrum Dresden-Rossendorf

  - positron energy adjustable in the range 0.027 – 36 keV

    W. Anwand et al., Defect and Diffusion Forum 331, 25 (2012)

- **fast positrons with continuos energy spectrum**

  - ^{68}Ge/^{68}Ga positron generator, $T_{+,max}$ = 1897 keV

  - pair production from bremsstrahlung radiation (GiPS), $T_{+,max}$ = 16 MeV

  - ELBE, Helmholtz Zentrum Dresden-Rossendorf

    M. Butterling et al., Nucl. Instrum. Methods B 269, 2623 (2011)

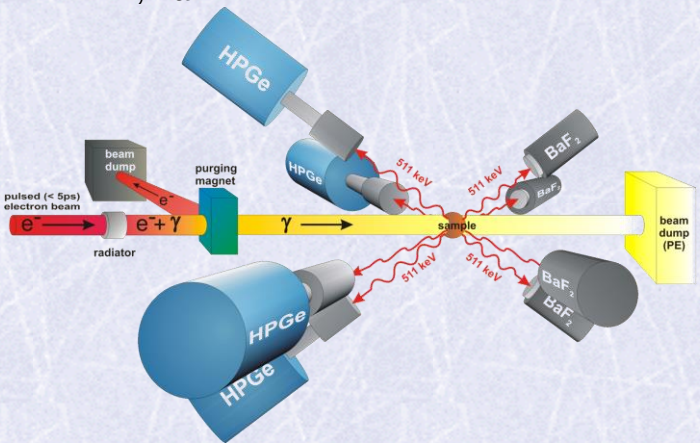

CDB spectra – monoenergetic slow positrons

- monoenergetic slow positrons, T_+ = 35 keV
- thick Fe target (thickness 0.5 mm)

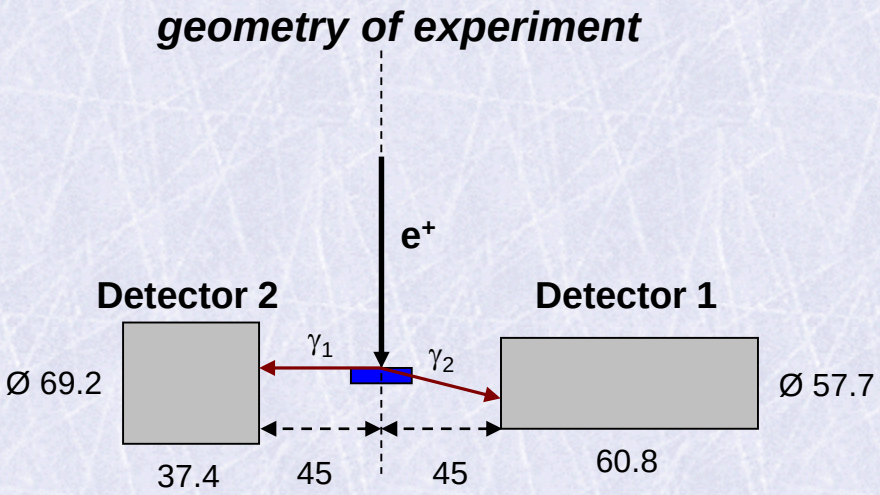

CDB spectra – monoenergetic slow positrons

- monoenergetic slow positrons, T_+ = 35 keV
- thick Fe target (thickness 0.5 mm)

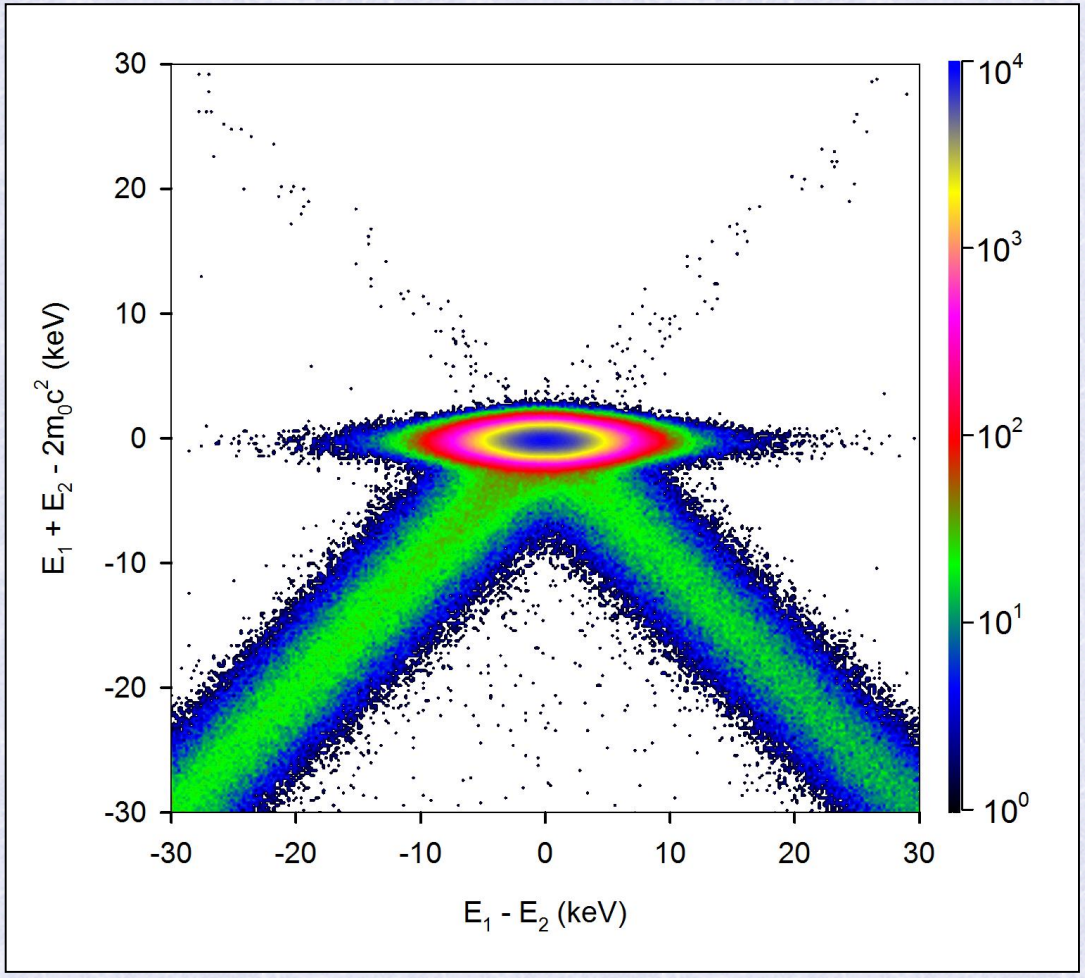

CDB spectrum:
sum of energies of annihilation gamma rays

$$E_1 + E_2 - 2m_0c^2$$

plotted versus
difference of these energies

$$E_1 - E_2$$

CDB spectra – monoenergetic slow positrons

- monoenergetic slow positrons, T_+ = 35 keV
- thick Fe target (thickness 0.5 mm)

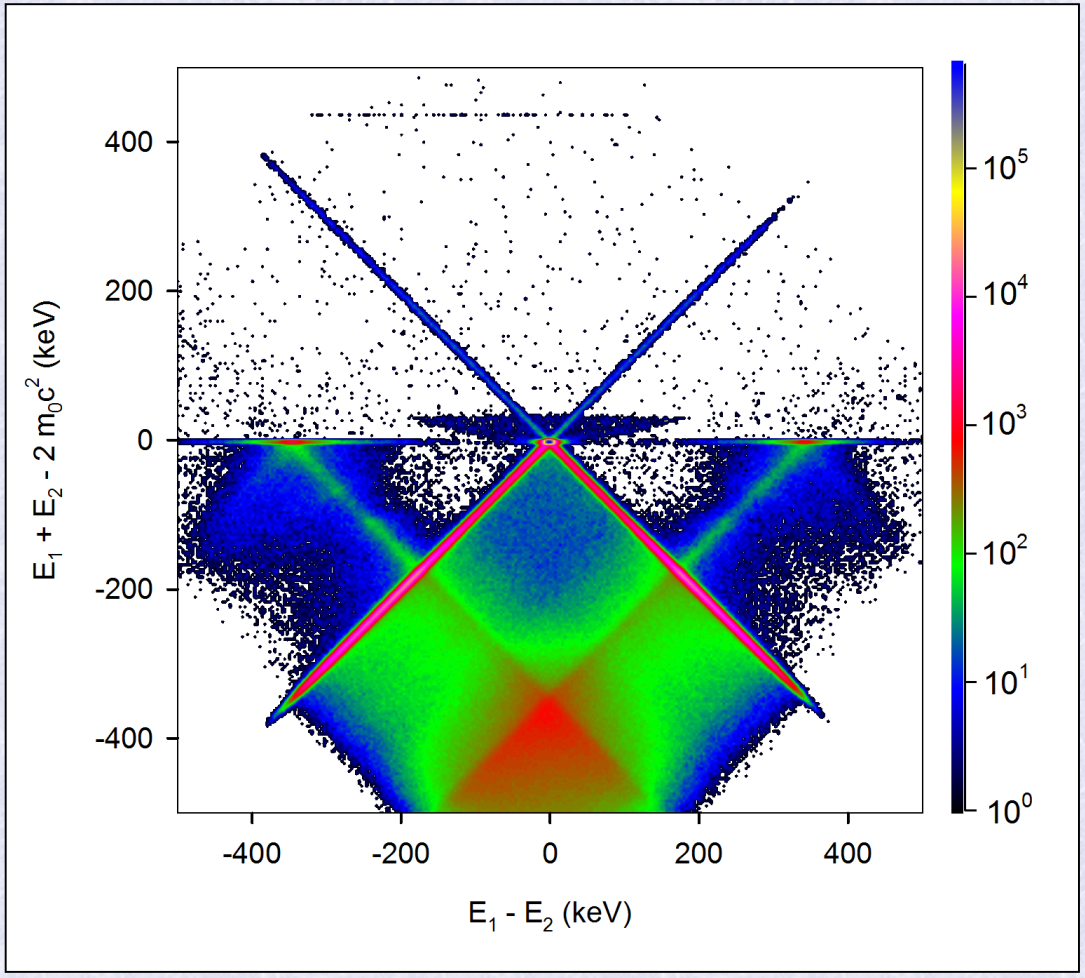

CDB spectra – monoenergetic slow positrons

- monoenergetic slow positrons, T_+ = 35 keV
- thick Fe target (thickness 0.5 mm)

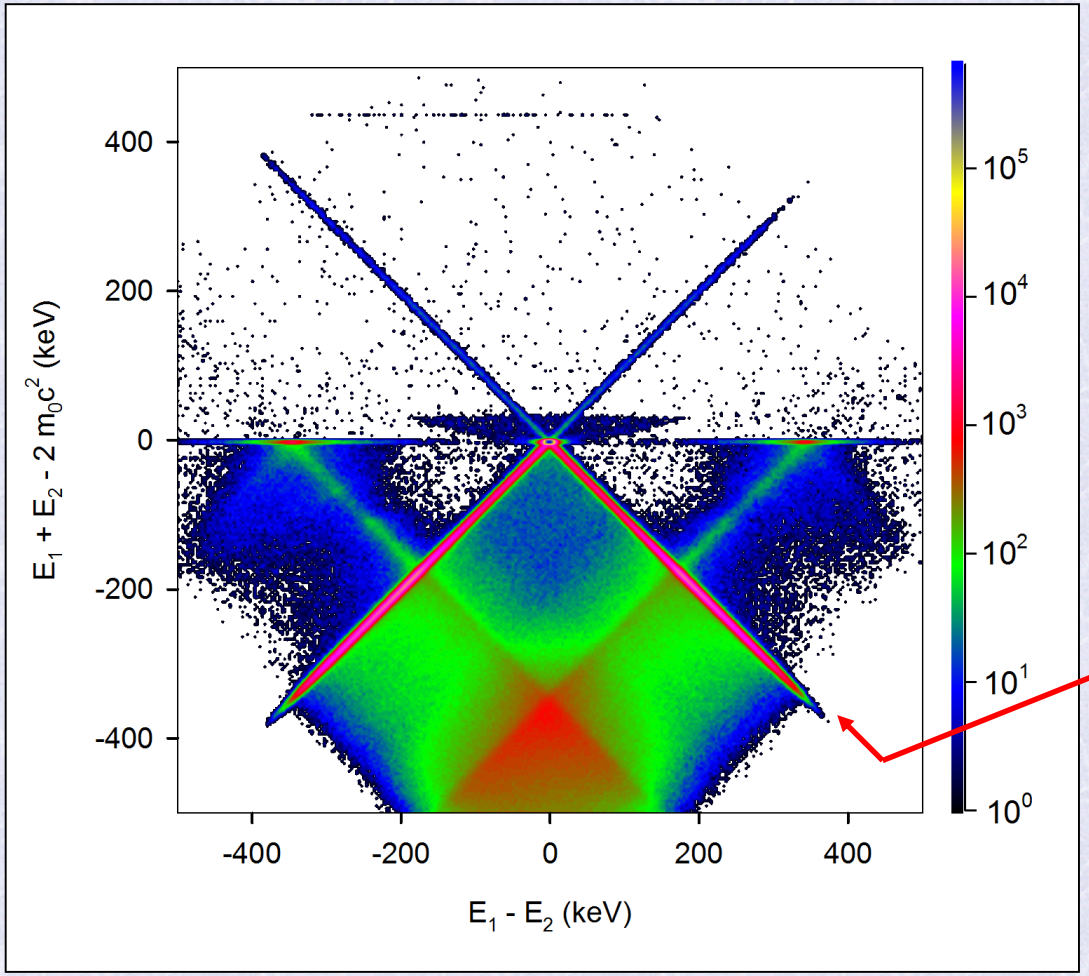

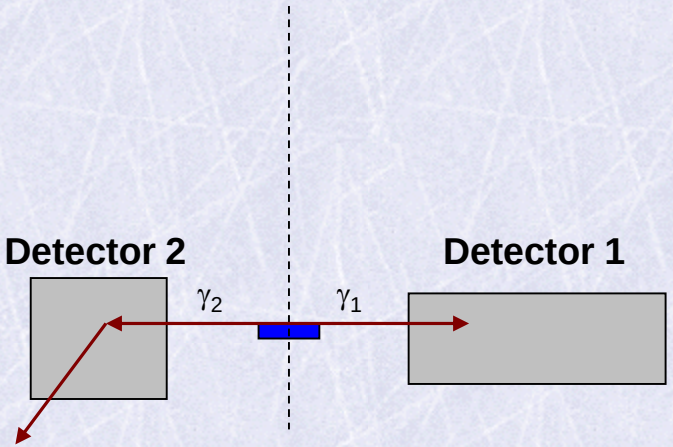

Compton scattering of one annihilation γ-ray

CDB spectra – monoenergetic slow positrons

- monoenergetic slow positrons, T_+ = 35 keV
- thick Fe target (thickness 0.5 mm)

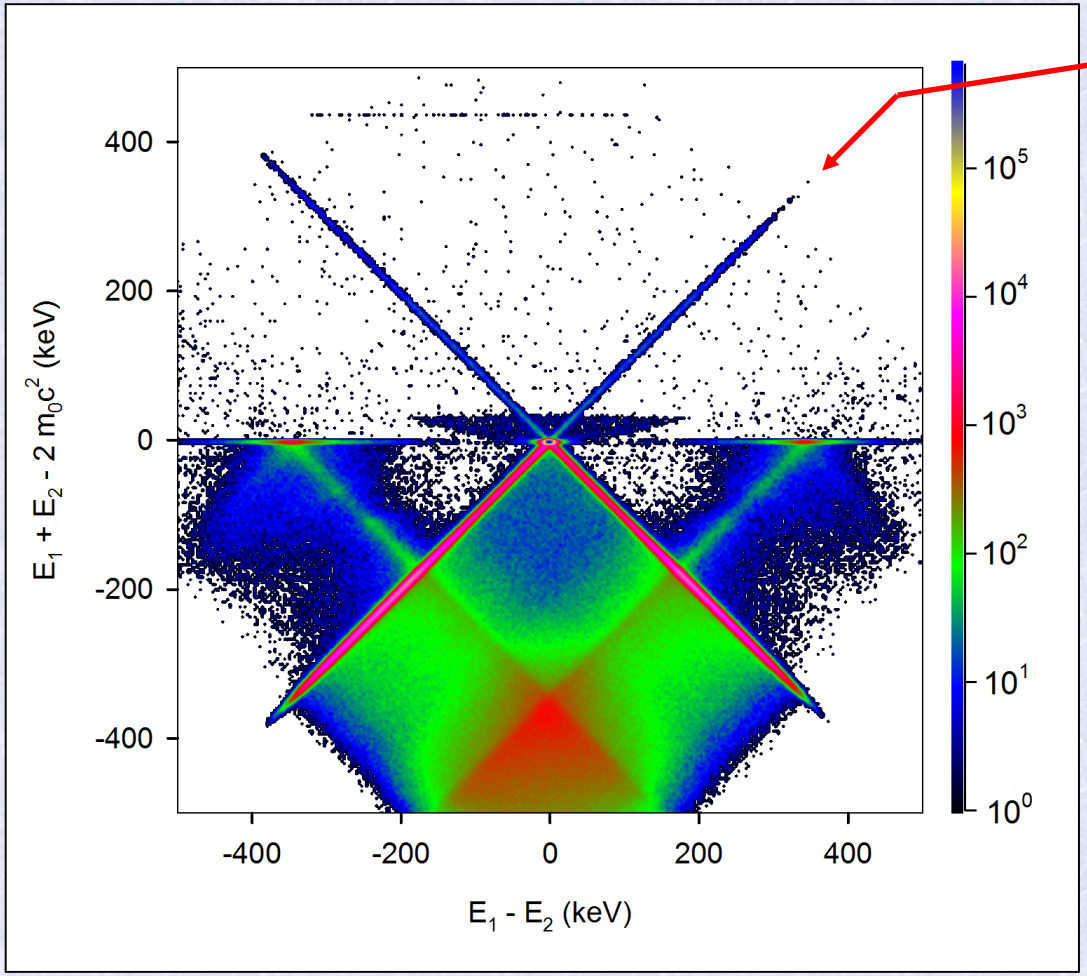

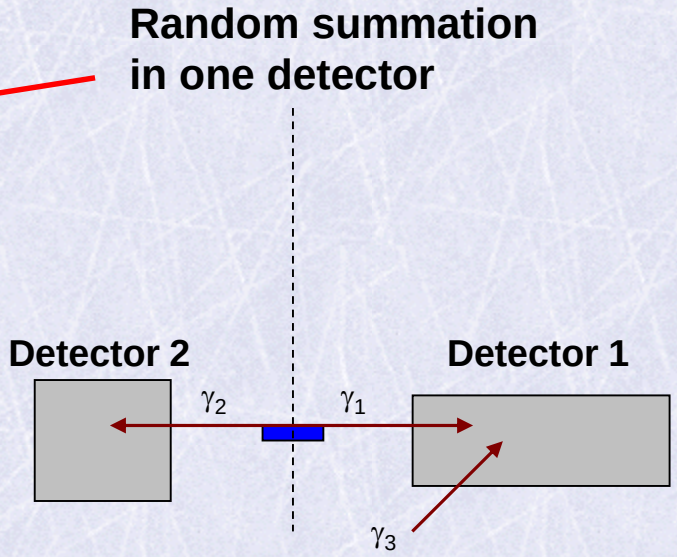

CDB spectra – monoenergetic slow positrons

- monoenergetic slow positrons, T_+ = 35 keV
- thick Fe target (thickness 0.5 mm)

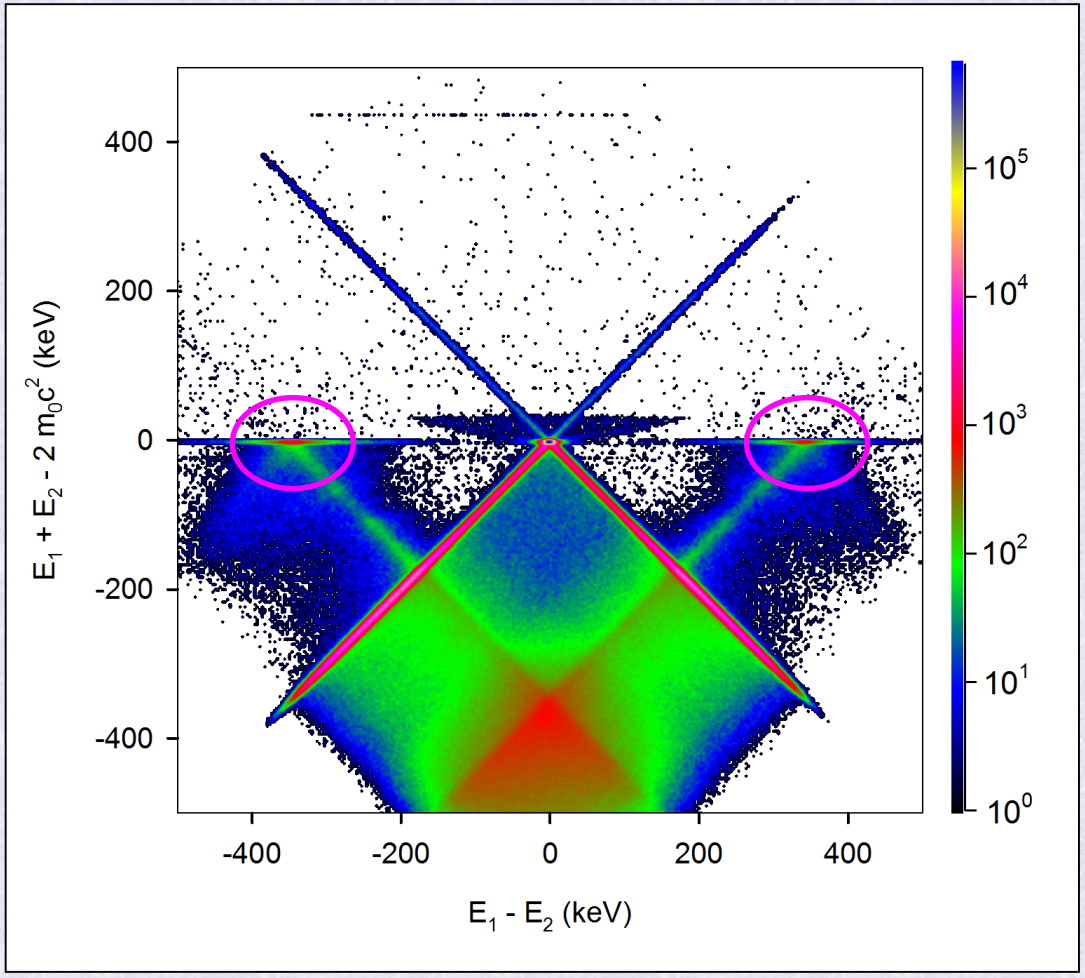

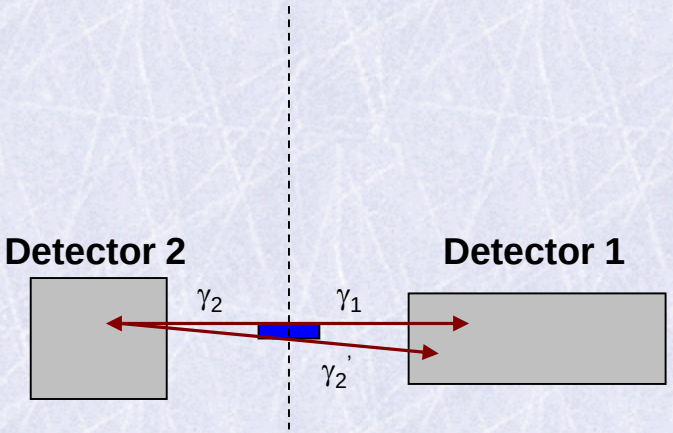

Back-scattering of one annihilation γ-ray

CDB spectra – monoenergetic slow positrons

- monoenergetic slow positrons, T_+ = 35 keV
- thick Fe target (thickness 0.5 mm)

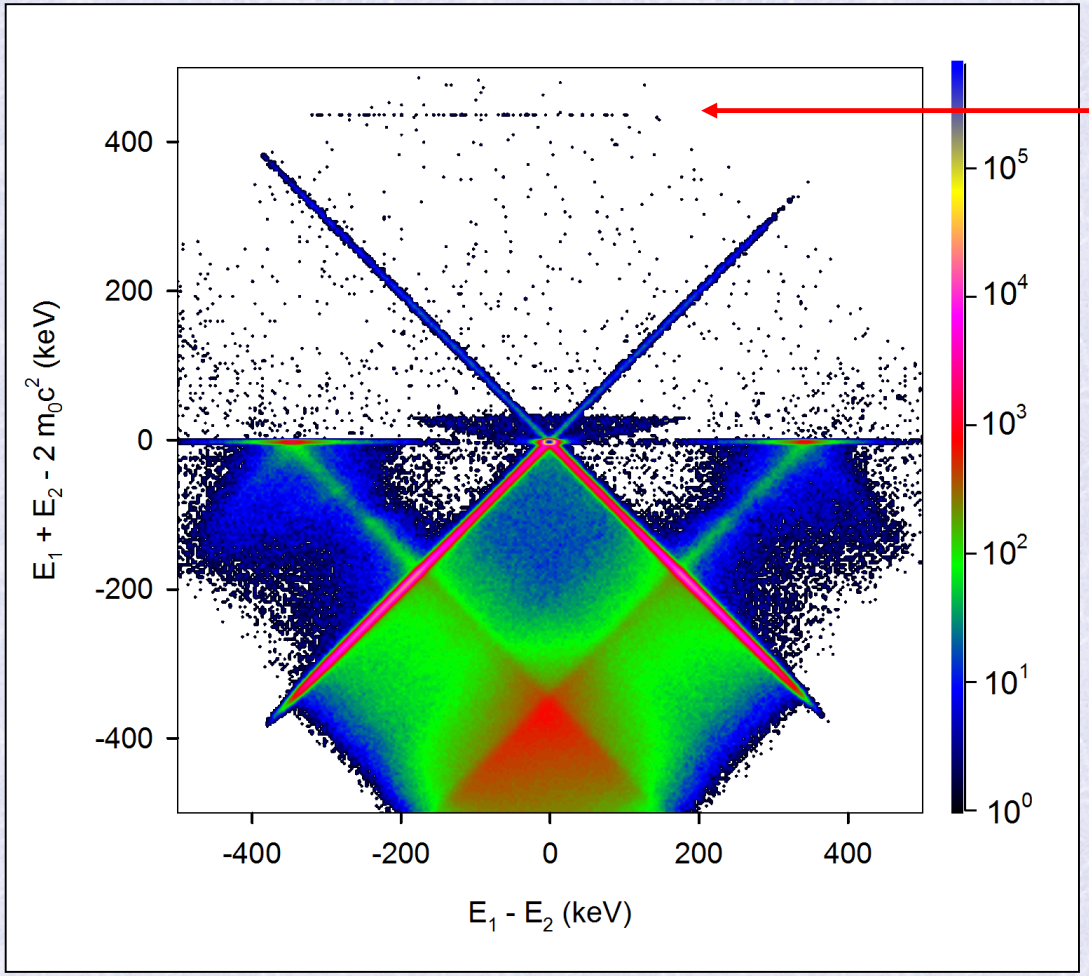

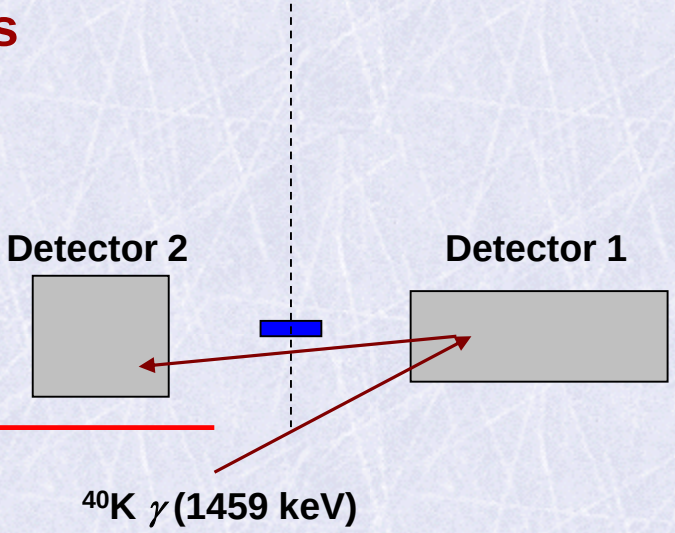

scattering of ^{40}K γ-ray from background

CDB spectra – monoenergetic slow positrons

- monoenergetic slow positrons, T_+ = 35 keV
- thick Fe target (thickness 0.5 mm)

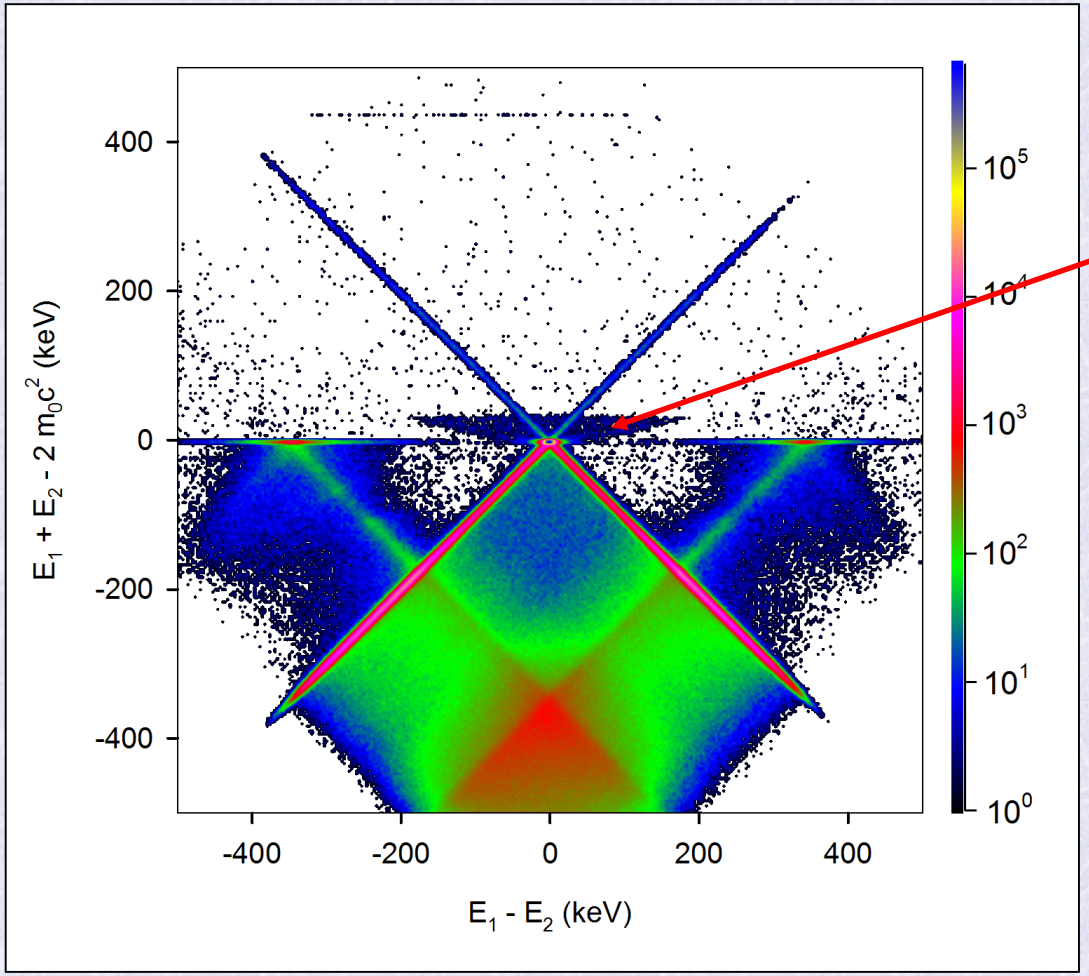

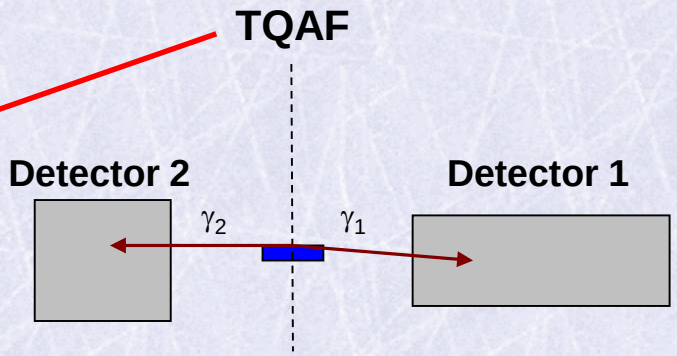

CDB spectra – monoenergetic slow positrons

- monoenergetic slow positrons, T_+ = 35 keV
- thick Fe target (thickness 0.5 mm)

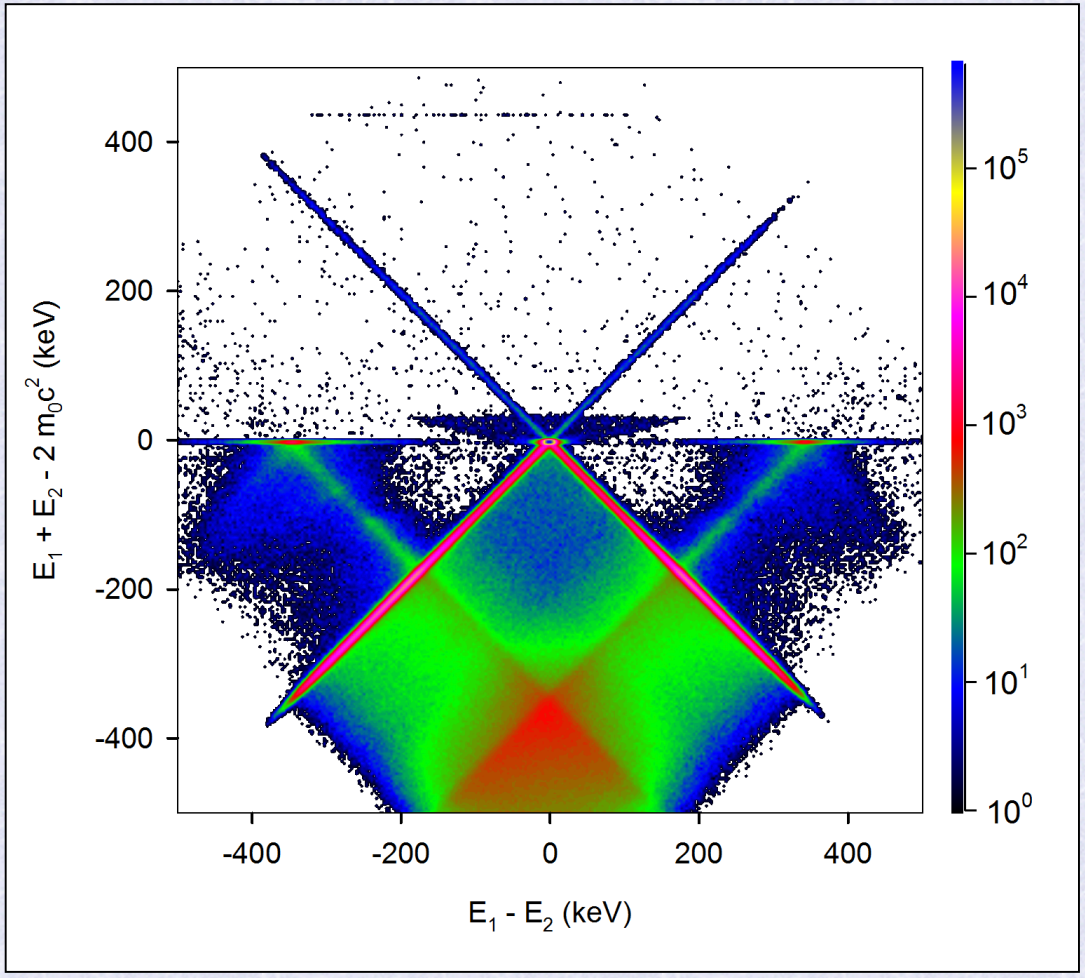

TQAF

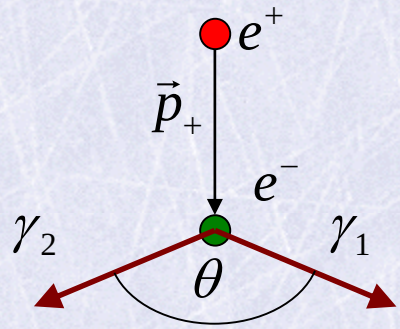

conservation of energy & momentum

$$\frac{1}{E_1}+\frac{1}{E_2}=\frac{1-\cos\theta}{m_0c^2}$$

CDB spectra – monoenergetic slow positrons

$$E_1 + E_2 - 2m_0c^2 = \sqrt{(E_1 - E_2)^2 + \left(\frac{2m_0c^2}{1-\cos\theta}\right)^2} + \frac{2m_0c^2\cos\theta}{1-\cos\theta}$$

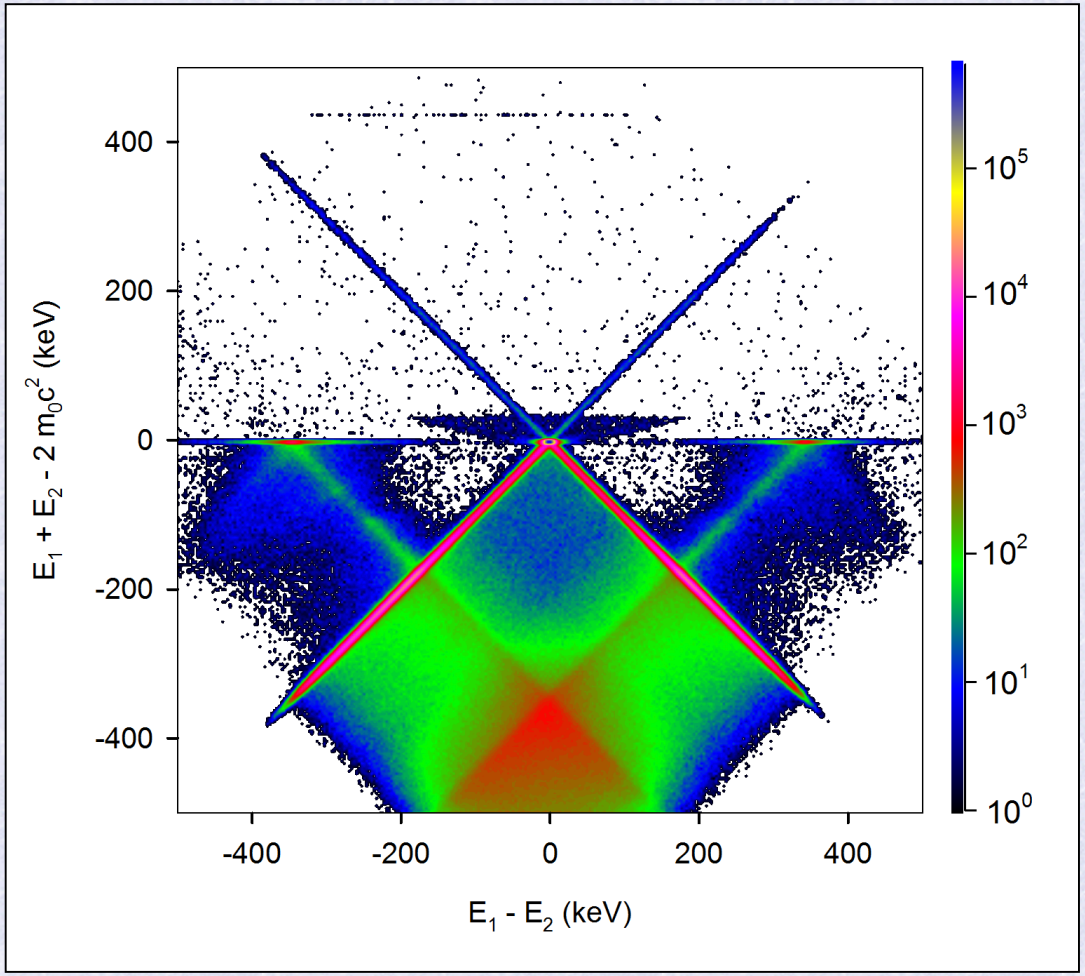

TQAF

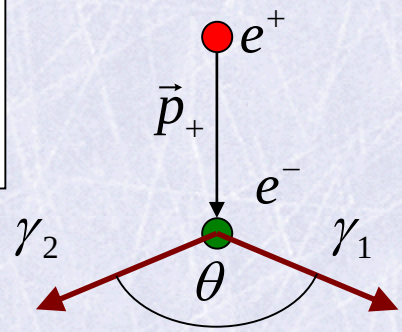

conservation of energy & momentum

$$\frac{1}{E_1} + \frac{1}{E_2} = \frac{1-\cos\theta}{m_0c^2}$$

CDB spectra – monoenergetic slow positrons

$$E_1 + E_2 - 2m_0c^2 = \sqrt{(E_1 - E_2)^2 + \left(\frac{2m_0c^2}{1-\cos\theta}\right)^2} + \frac{2m_0c^2\cos\theta}{1-\cos\theta}$$

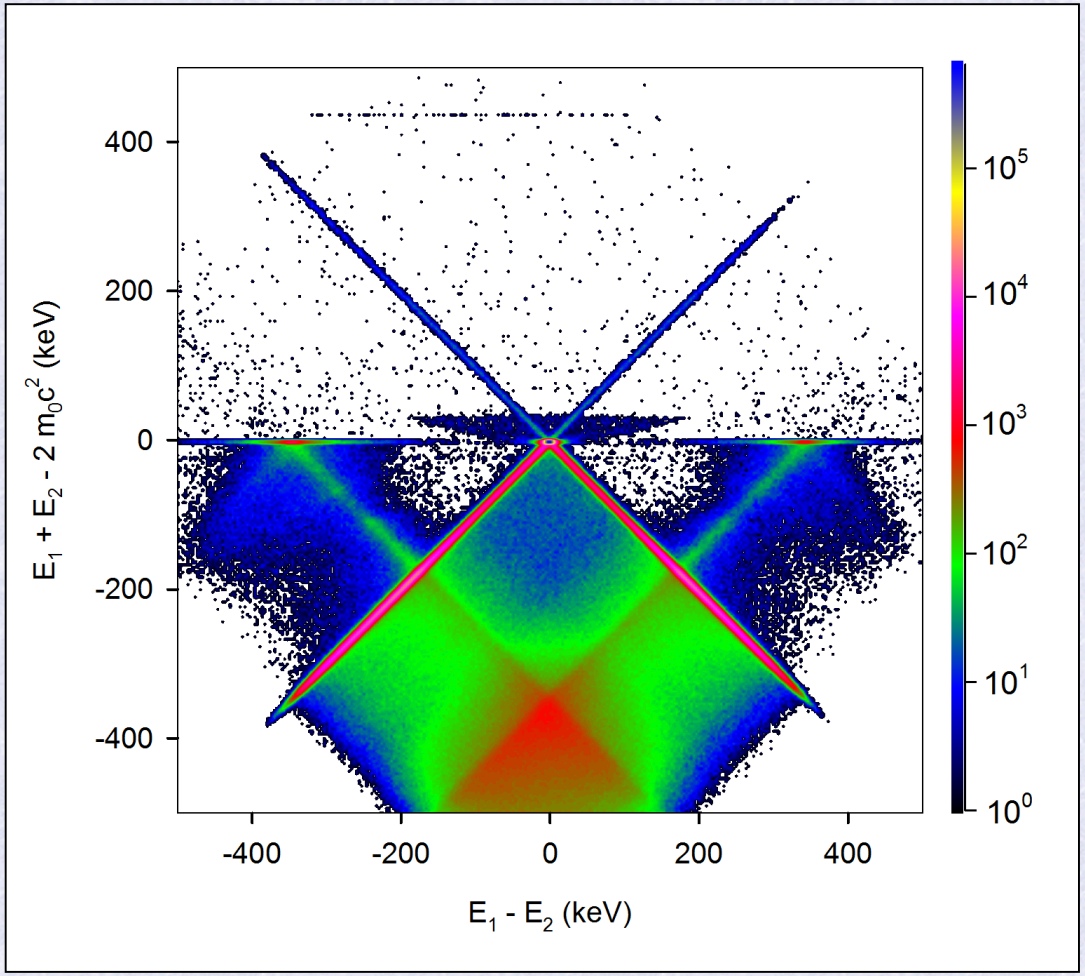

TQAF

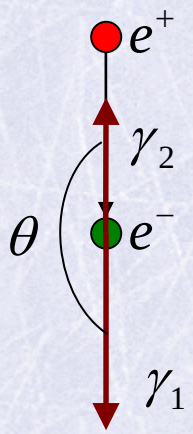

maximum energy difference for anti-collinear γ-rays

$\theta = 180^{o}$

for T_+ = 35 keV

$-192\ \text{keV} \le E_1 - E_2 \le 192\ \text{keV}$

CDB spectra – monoenergetic slow positrons

$$E_1 + E_2 - 2m_0c^2 = \sqrt{(E_1 - E_2)^2 + (m_0c^2)^2} - m_0c^2$$

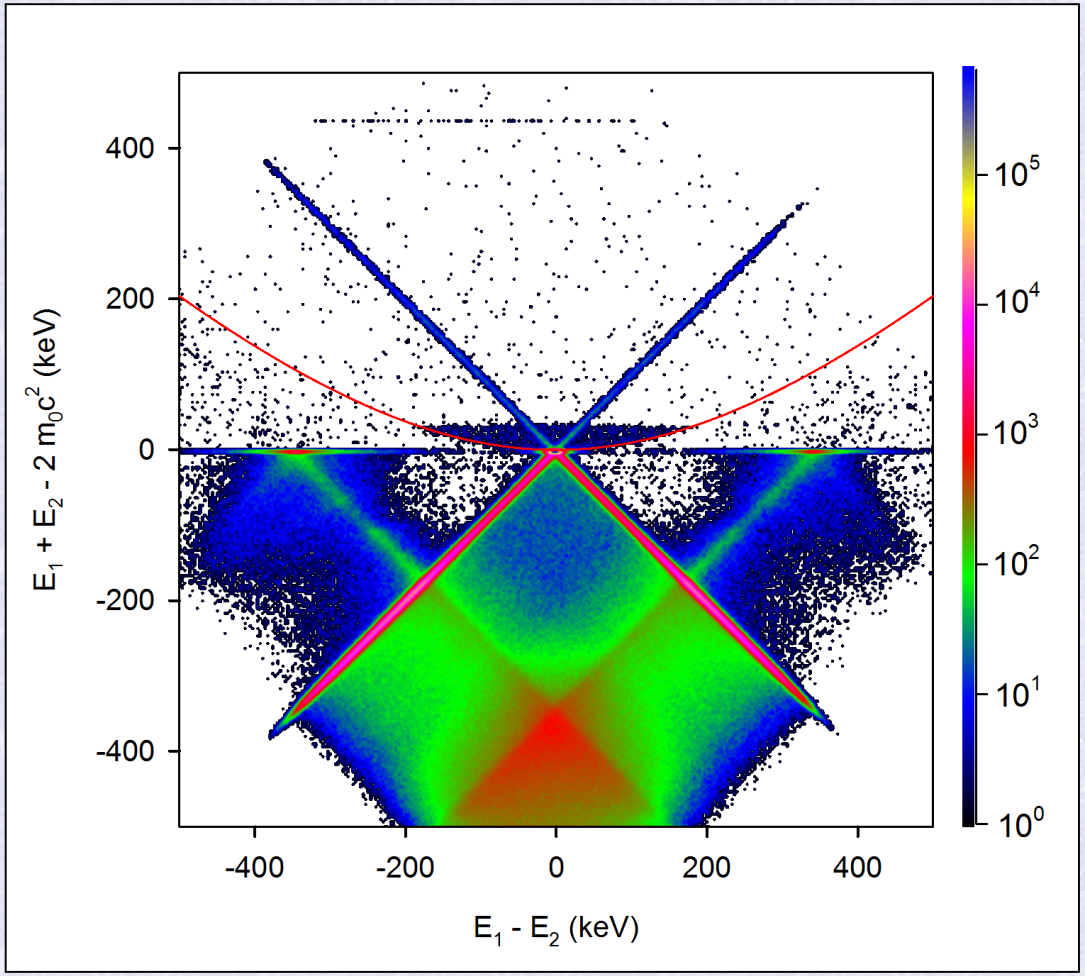

TQAF

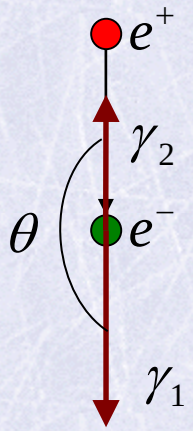

maximum energy difference for anti-collinear γ-rays

$\theta = 180^{o}$

for T_+ = 35 keV

$-192\ \text{keV} \le E_1 - E_2 \le 192\ \text{keV}$

CDB spectra – monoenergetic slow positrons

- monoenergetic slow positrons, T_+ = 35 keV
- thick Fe target (thickness 0.5 mm)

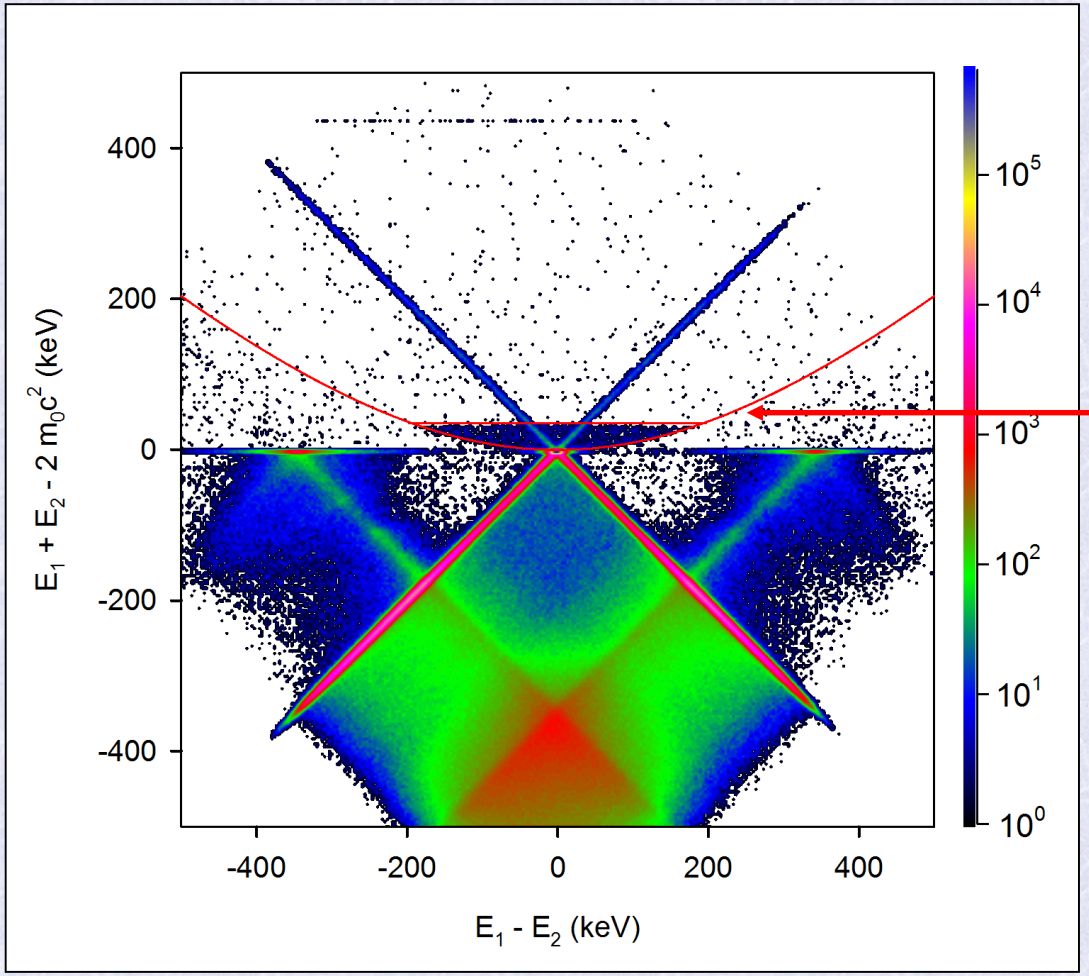

TQAF

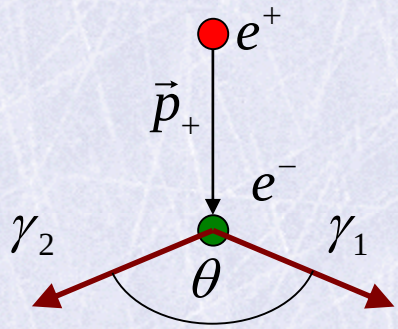

kinematical cut-off
T_+ = 35 keV

$$E_1 + E_2 - 2m_0c^2 \leq T_+$$

CDB spectra – monoenergetic slow positrons

- monoenergetic slow positrons, T_+ = 35 keV
- thick Fe target (thickness 0.5 mm)

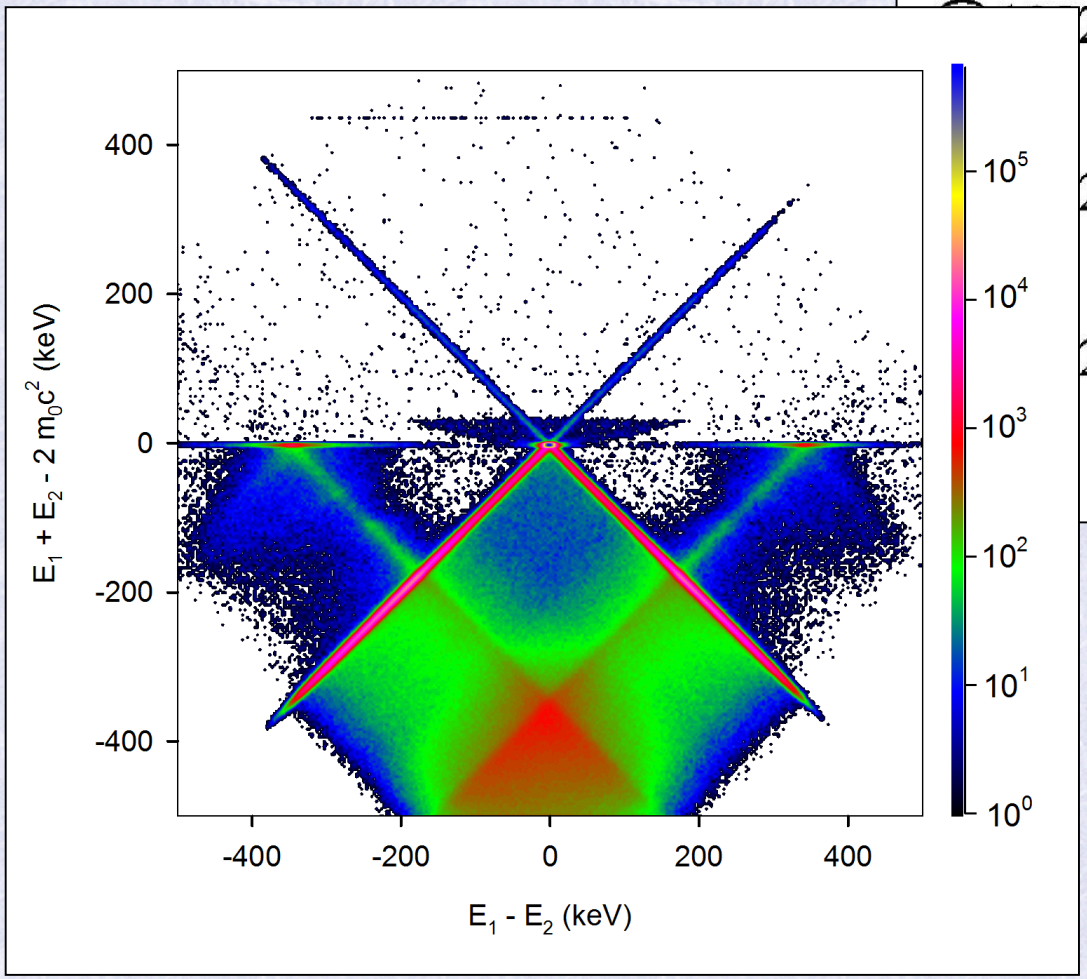

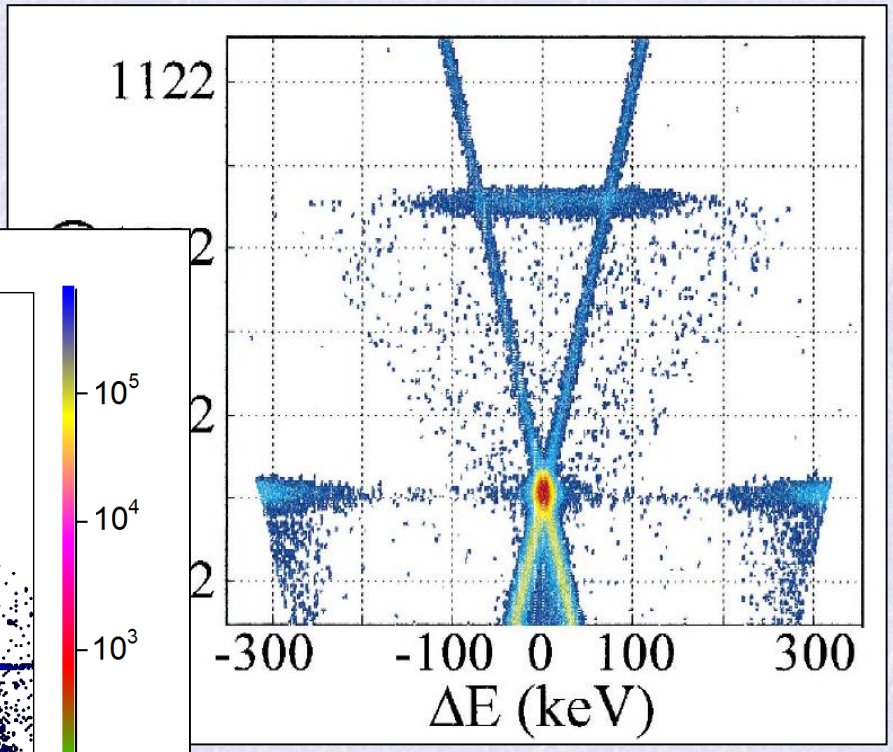

- T_+ = 70 keV
- thin Al target
- thickness 0.8 μm

A. W. Hunt, M.H. Weber,
J.A. Golovchenko, K.G. Lynn,
Appl. Surf. Sci. 149, 282 (1999)

CDB spectra – monoenergetic slow positrons

- thick Fe target (thickness 0.5 mm)
- **TQAF disappears for slow positrons → benchmark test of slow positron beams**

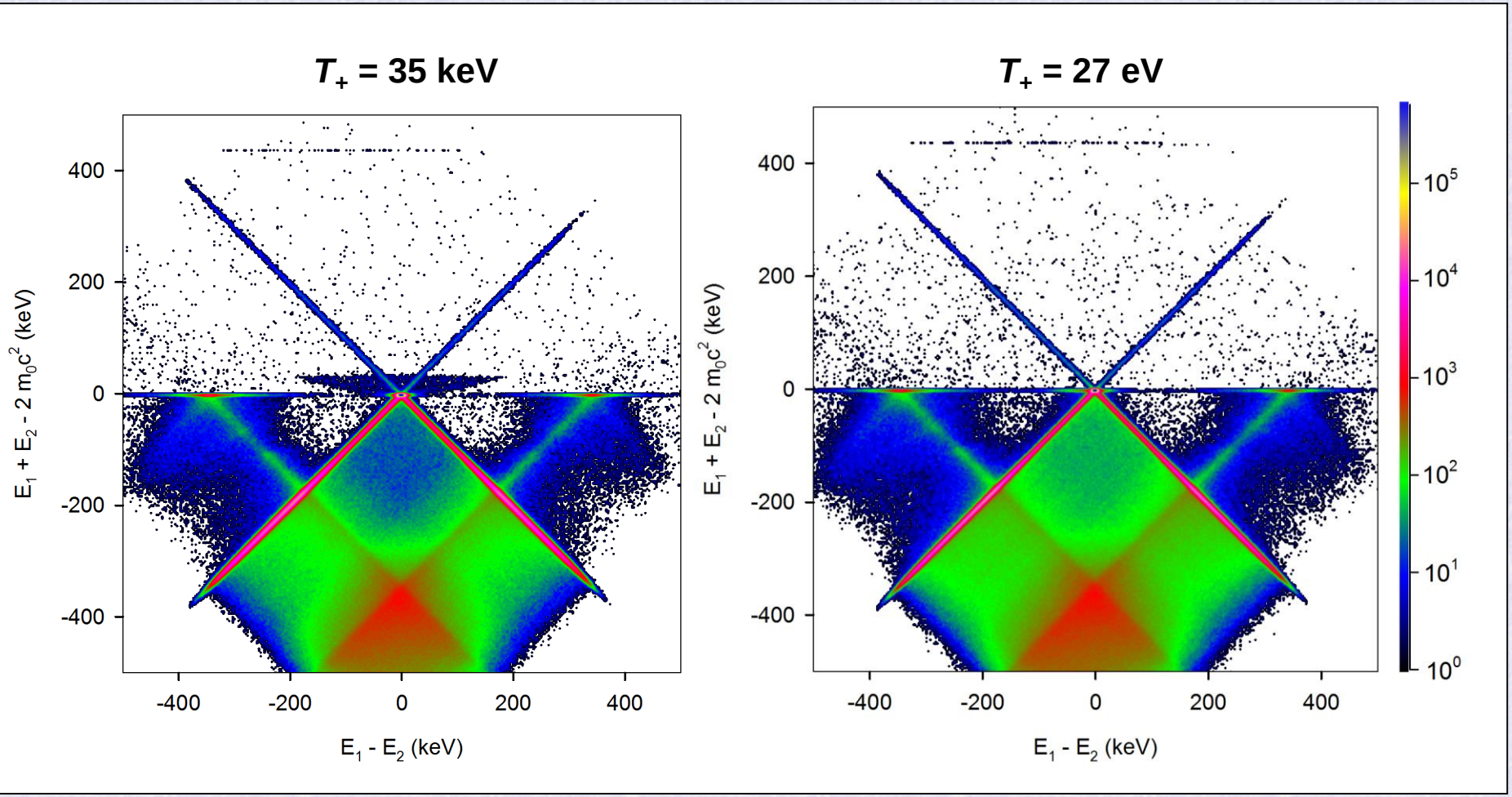

CDB spectra – monoenergetic slow positrons

- thick Fe target (thickness 0.5 mm)
- vertical cut integrated in the range $-192\ \mathrm{keV} < E_1 - E_2 < 192\ \mathrm{keV}$

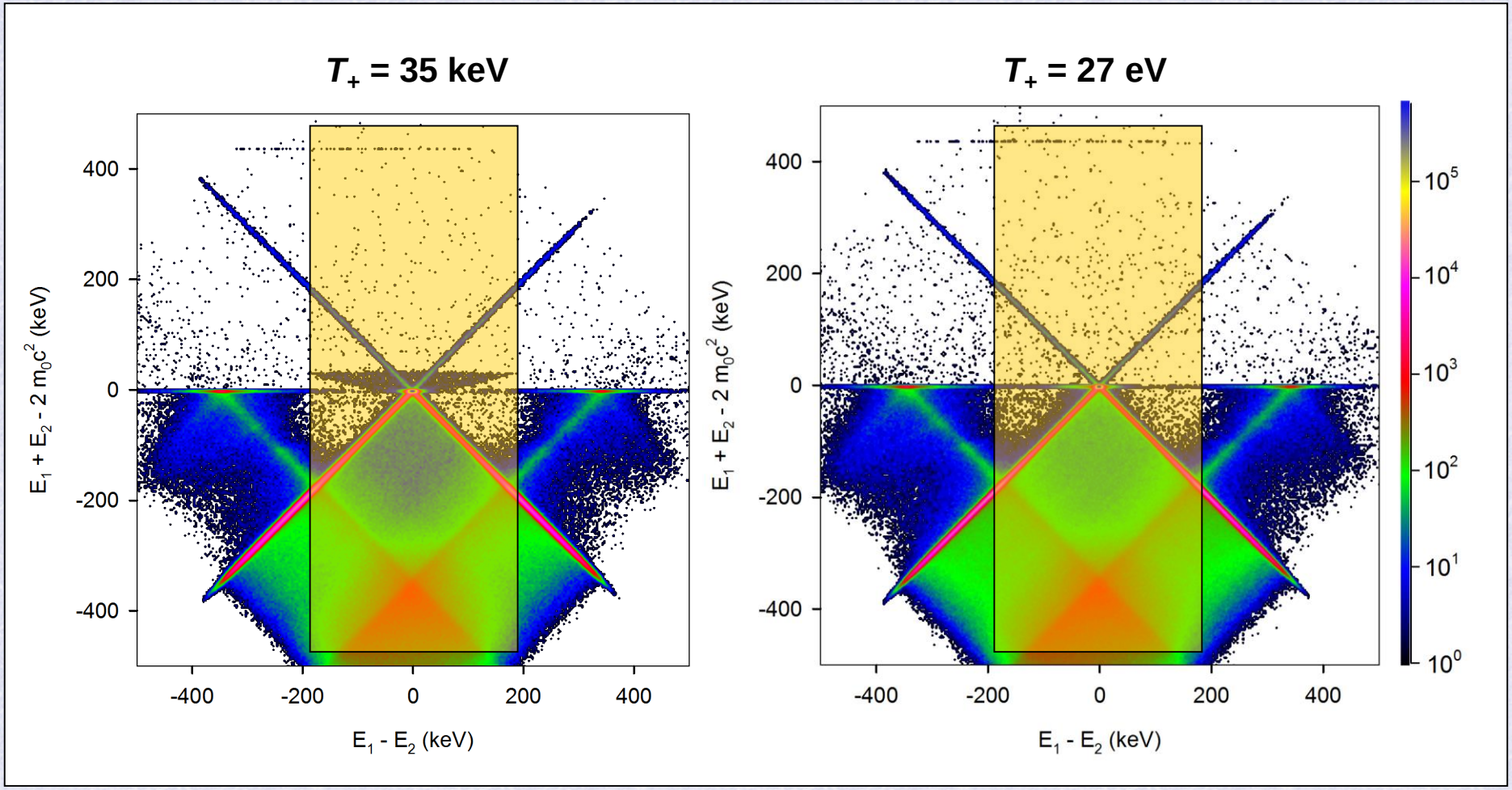

CDB spectra – monoenergetic slow positrons

- thick Fe target (thickness 0.5 mm)
- vertical cut integrated in the range $-192\ \mathrm{keV} < E_1 - E_2 < 192\ \mathrm{keV}$

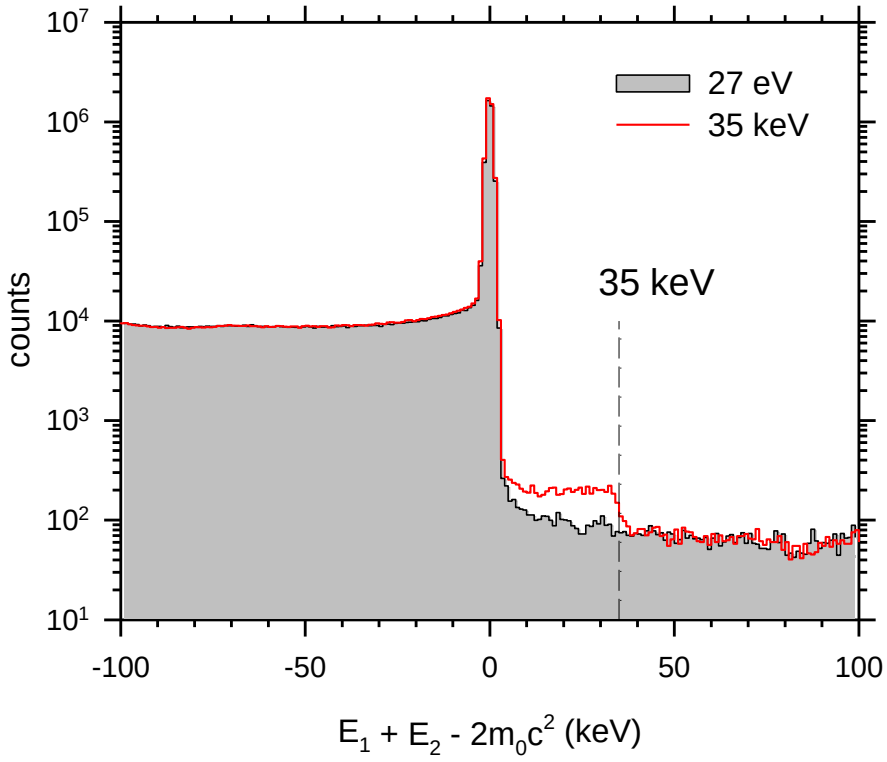

CDB spectra – monoenergetic slow positrons

- thick Fe target (thickness 0.5 mm)
- vertical cut integrated in the range $-192\ \mathrm{keV} < E_1 - E_2 < 192\ \mathrm{keV}$

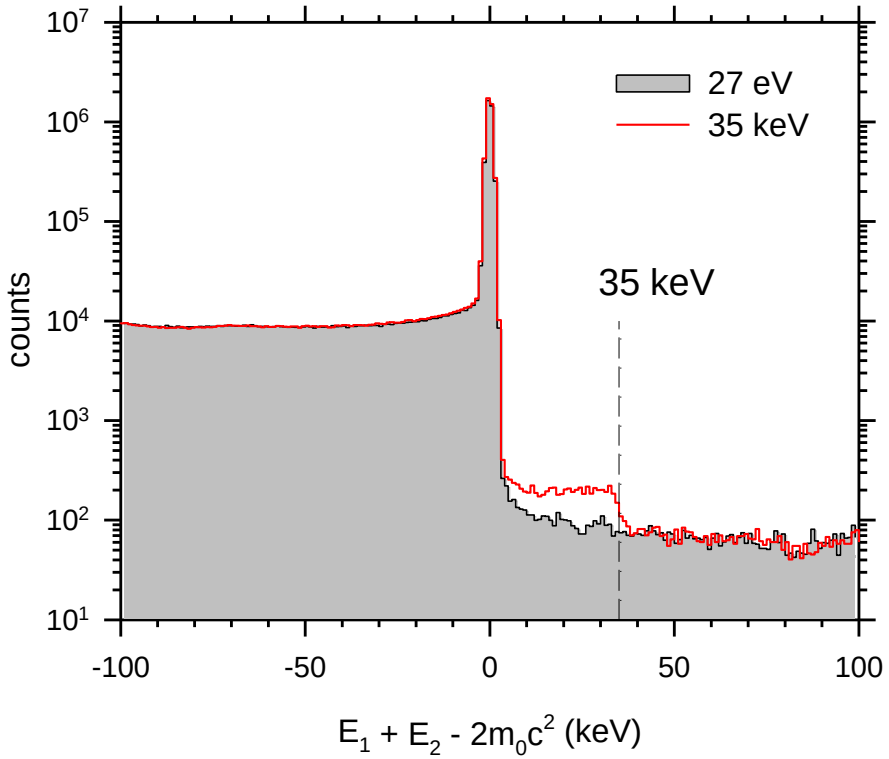

- probability of e^+ annihilation during slowing down from T_+ + dT_+ to T_+

$$dP(T_+) = -\frac{N_A \rho Z}{A} \frac{\sigma_{TQAF}(T_+)}{S(T_+)} dT_+$$

- e^+ stopping power

$$S(T_+) = \frac{dT_+}{dx} = \rho(a_1 Z + a_2) \frac{\gamma^{2.4}}{\gamma^{1.9} - 1}$$

$$\gamma = \frac{T_+ + m_0c^2}{m_0c^2} \qquad a_1 = -5.95\ \mathrm{g^{-1}cm^2keV} \qquad a_2 = 928\ \mathrm{g^{-1}cm^2keV}$$

R.K. Barta e al., Nucl. Phys.A 156, 314 (1970)

CDB spectra – monoenergetic slow positrons

- thick Fe target (thickness 0.5 mm)
- vertical cut integrated in the range $-192\ \mathrm{keV} < E_1 - E_2 < 192\ \mathrm{keV}$
- **TQAF in thick targets carries information about e^+ slowing down**

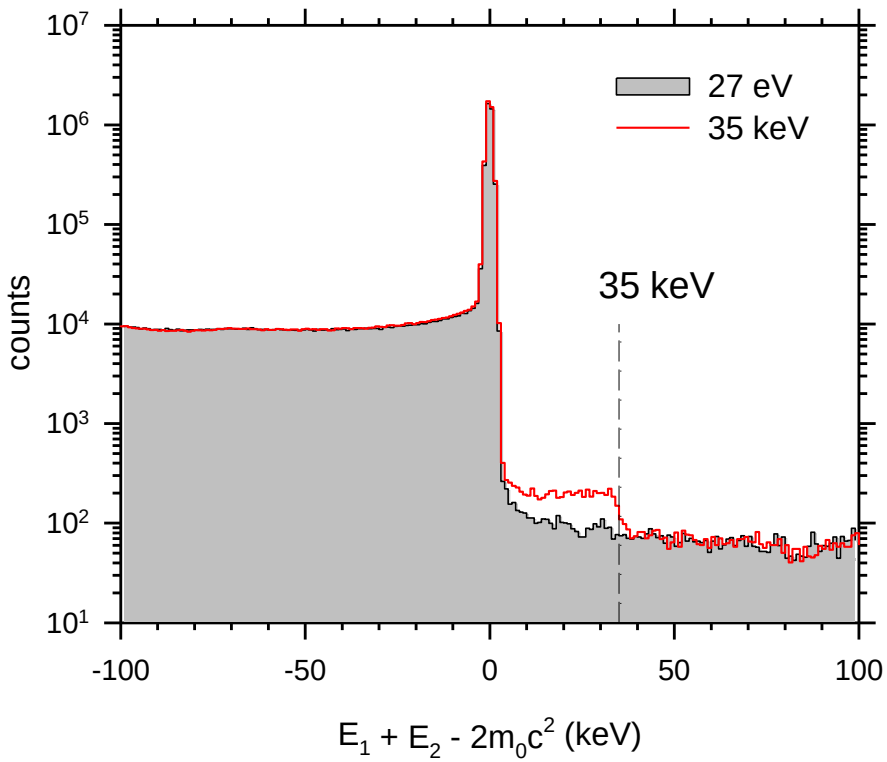

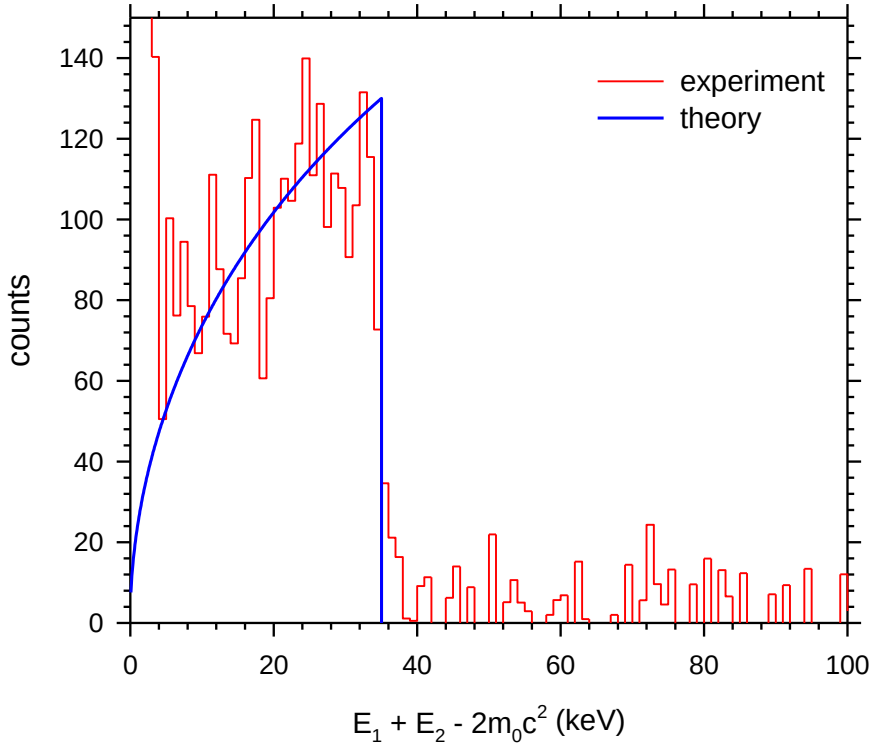

CDB spectra – monoenergetic slow positrons

- thick Fe target (thickness 0.5 mm)
- horizontal cut integrated in the range $5\,\mathrm{keV} < E_1 + E_2 - 2m_0c^2 < 35\,\mathrm{keV}$

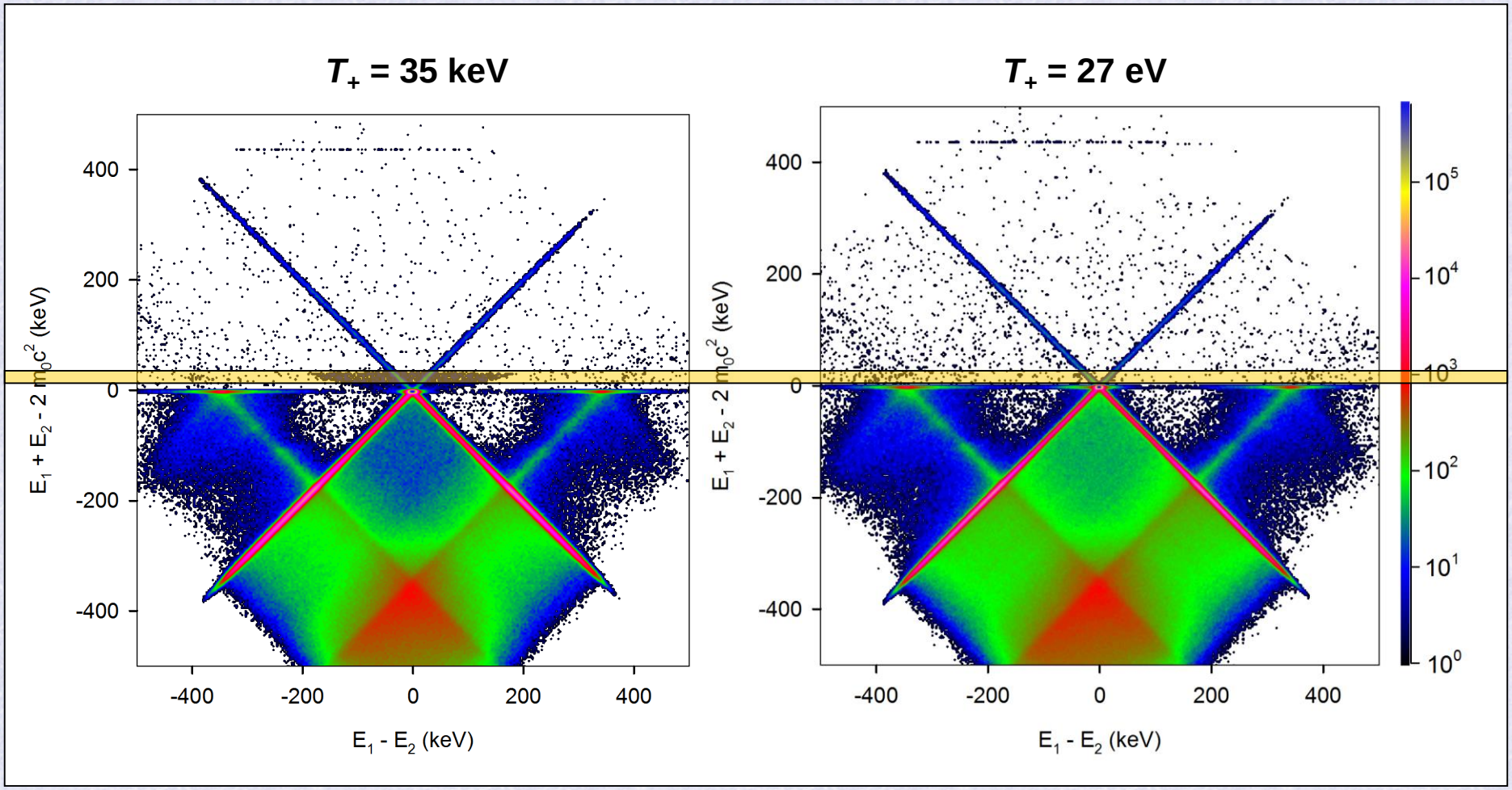

CDB spectra – monoenergetic slow positrons

- thick Fe target (thickness 0.5 mm)
- horizontal cut integrated in the range $5\,\mathrm{keV} < E_1 + E_2 - 2m_0c^2 < 35\,\mathrm{keV}$

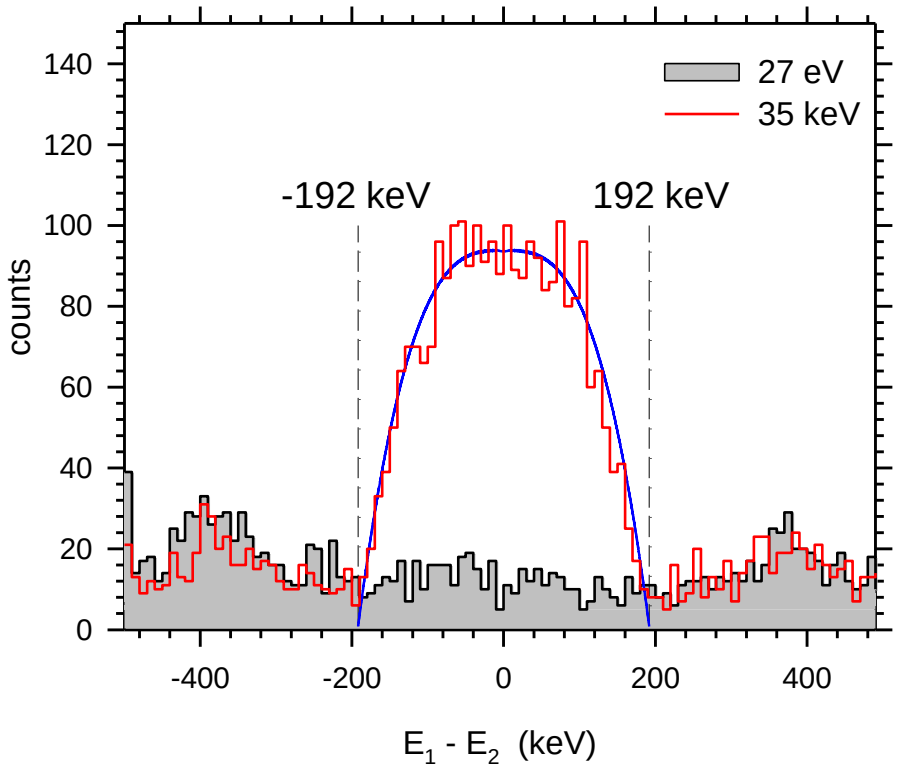

- probability of TQAF creating γ-rays with energy difference E_1 - E_2

$$P(E_1 - E_2) = -\frac{N_A \rho Z}{A} \int_{\sqrt{(E_1-E_2)^2 + (m_0c^2)^2} - m_0c^2}^{35\,\mathrm{keV}} \frac{\sigma_{TQAF}(T_+)}{S(T_+)} dT_+$$

- total probability of TQAF in Fe for positrons with energy of 35 keV

$$P_{TQAF} = 7.9 \times 10^{-4}$$

CDB spectra – monoenergetic slow positrons

- thick Fe target (thickness 0.5 mm)
- horizontal cut integrated in the range $5\,\mathrm{keV} < E_1 + E_2 - 2m_0c^2 < 35\,\mathrm{keV}$

$$P_{TQAF} = 7.9\times10^{-4}$$

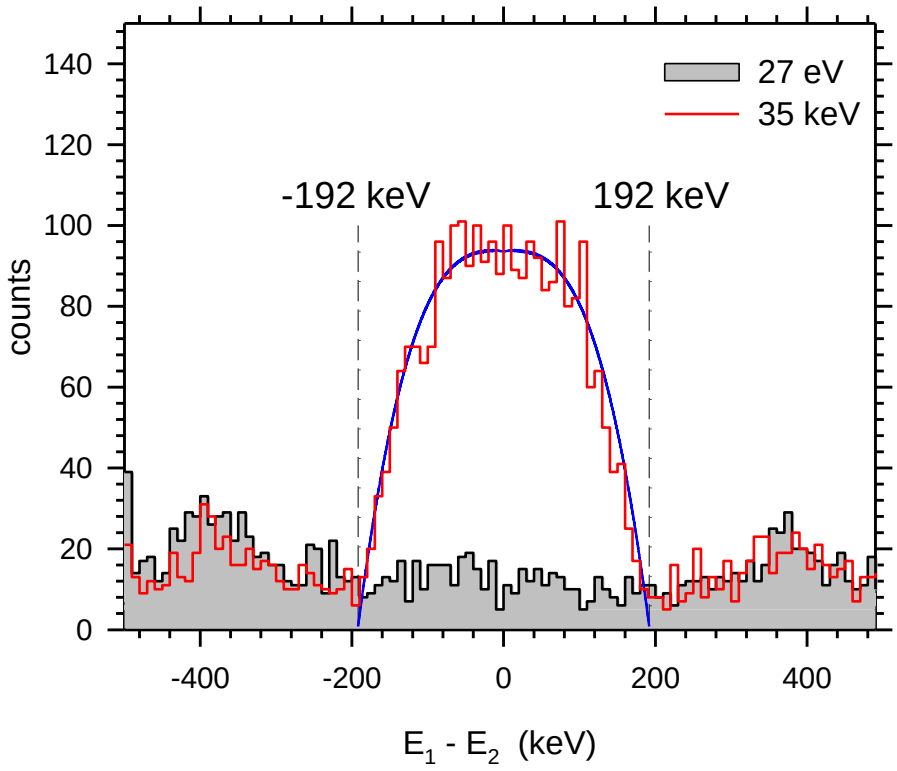

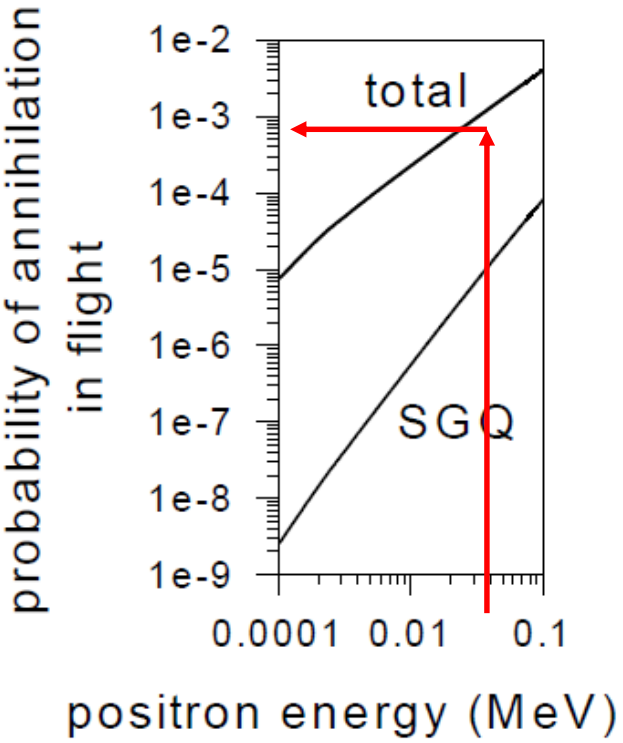

J. Dryzek et al., Proc. PSPA-33, 33 (2001)

CDB spectra – monoenergetic slow positrons

- thick Fe target (thickness 0.5 mm)

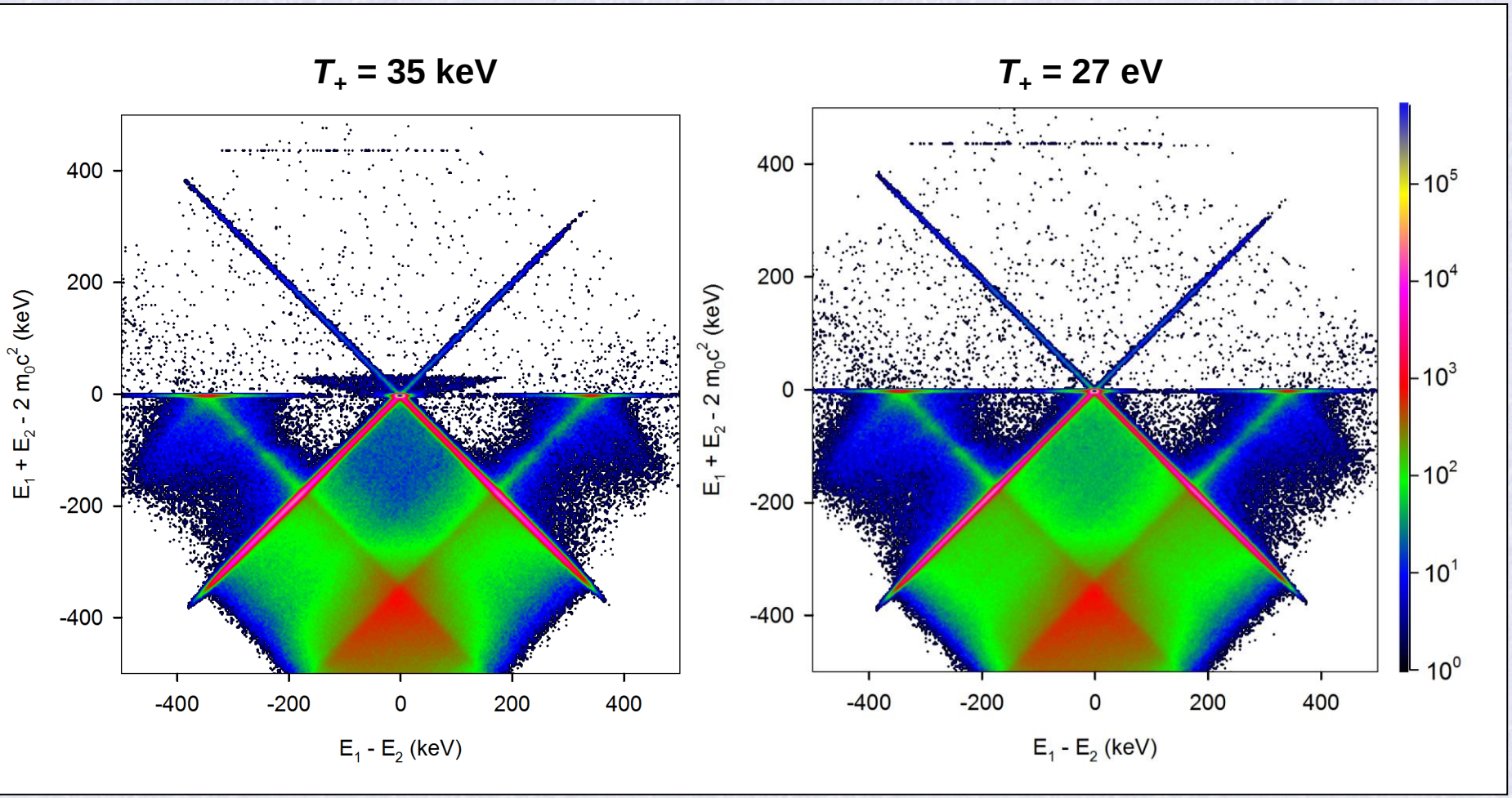

CDB spectra – monoenergetic slow positrons

- thick Fe target (thickness 0.5 mm)
- **3-γ o-Ps annihilations on the surface**

$$E_1 + E_2 + E_3 = 2m_0c^2$$

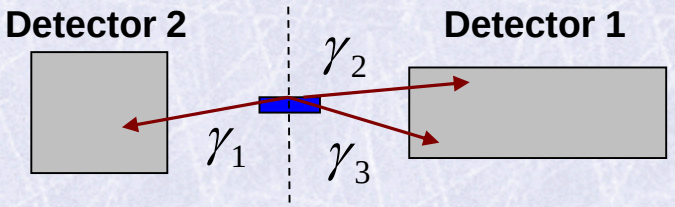

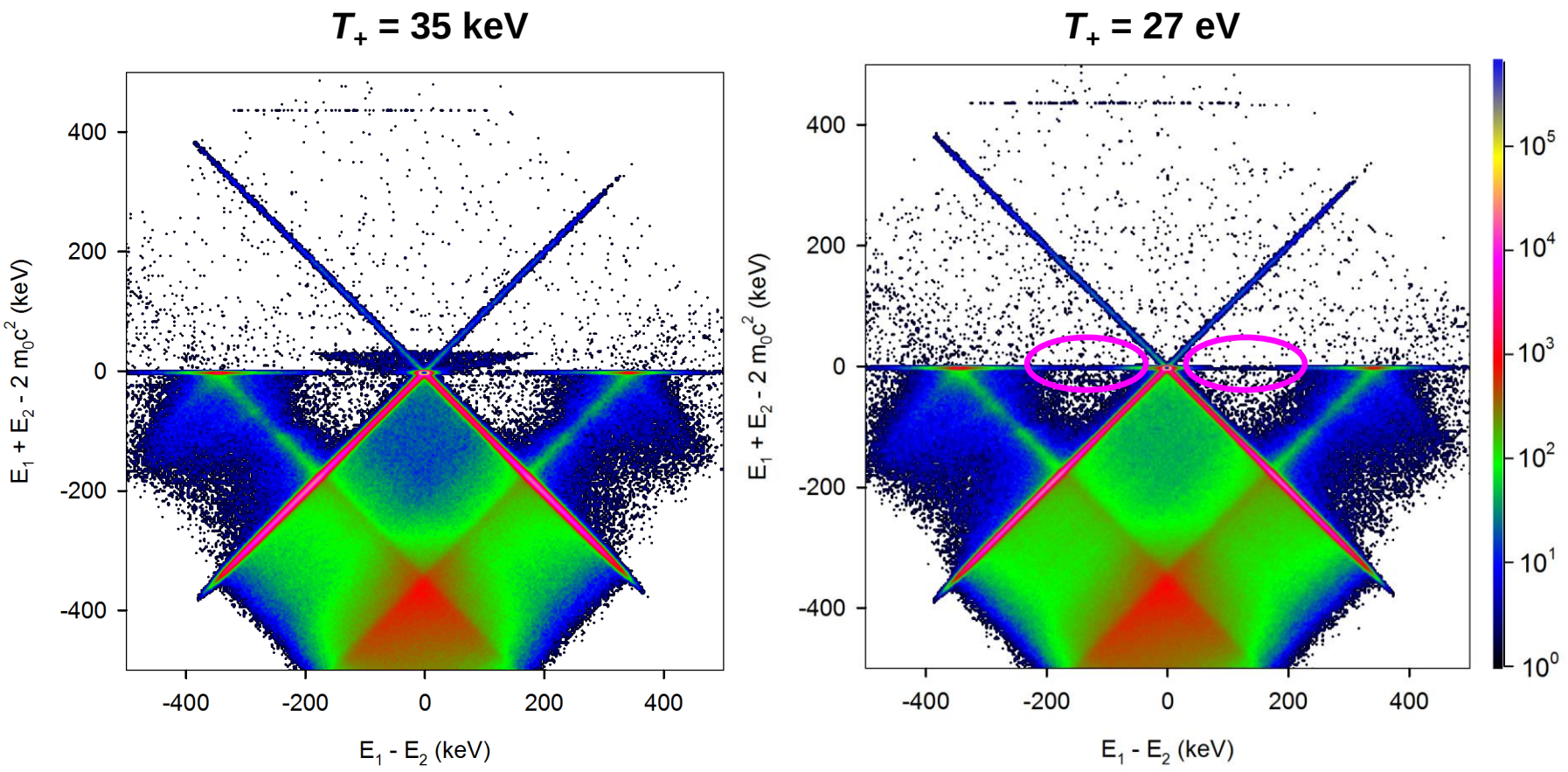

CDB spectra – monoenergetic slow positrons

- thick Fe target (thickness 0.5 mm)
- **3-γ o-Ps annihilations on the surface**

$$E_1 + E_2 + E_3 = 2m_0c^2$$

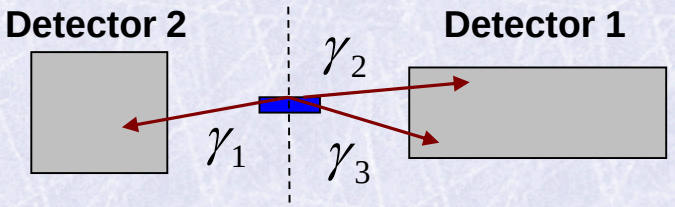

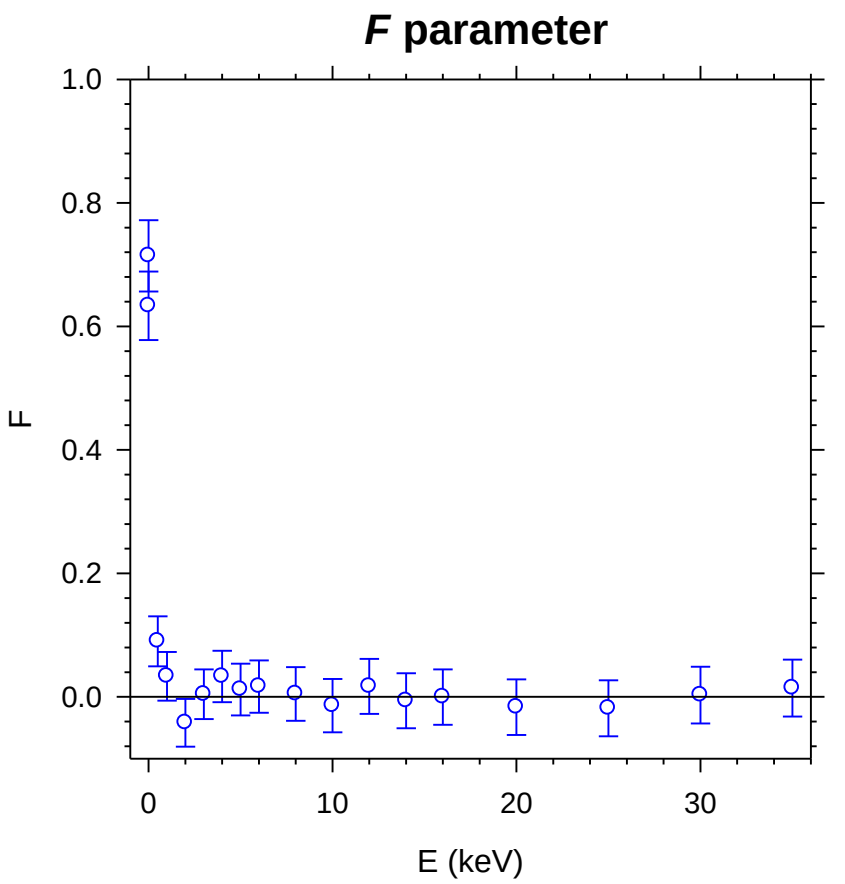

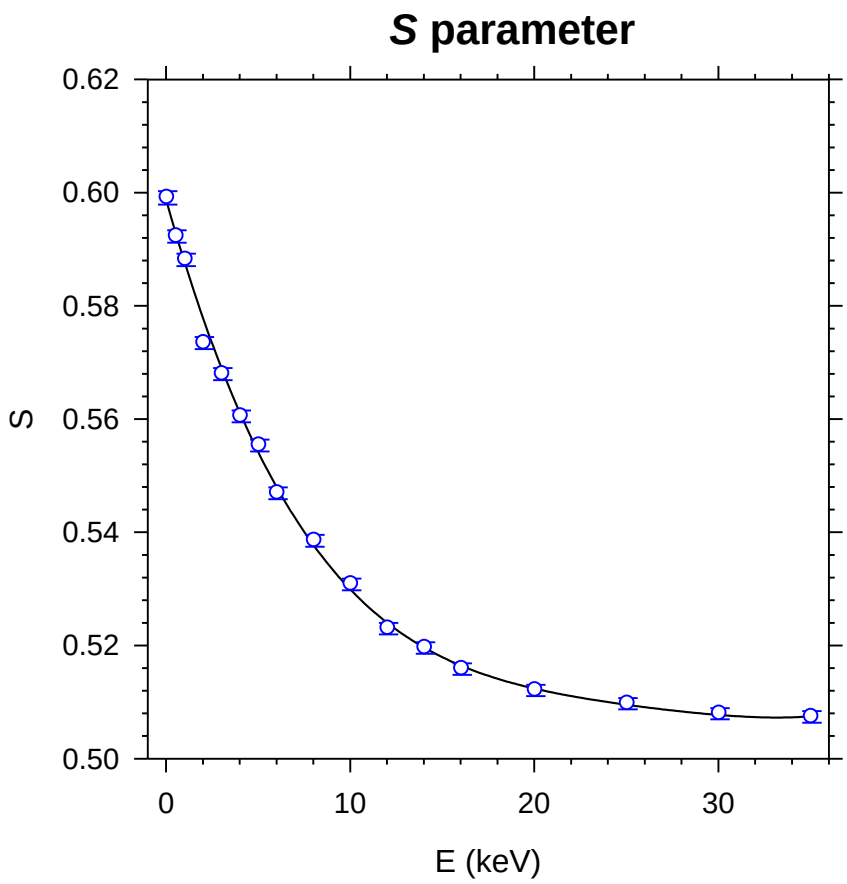

CDB spectra – fast positrons

- fast positrons, continuous energy spectrum

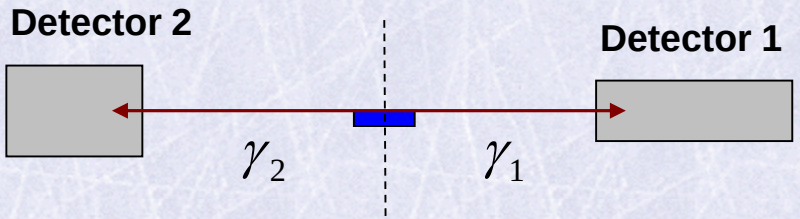

^{68}Ge/^{68}Ga, Mg target, $T_+ \leq 1897$ keV

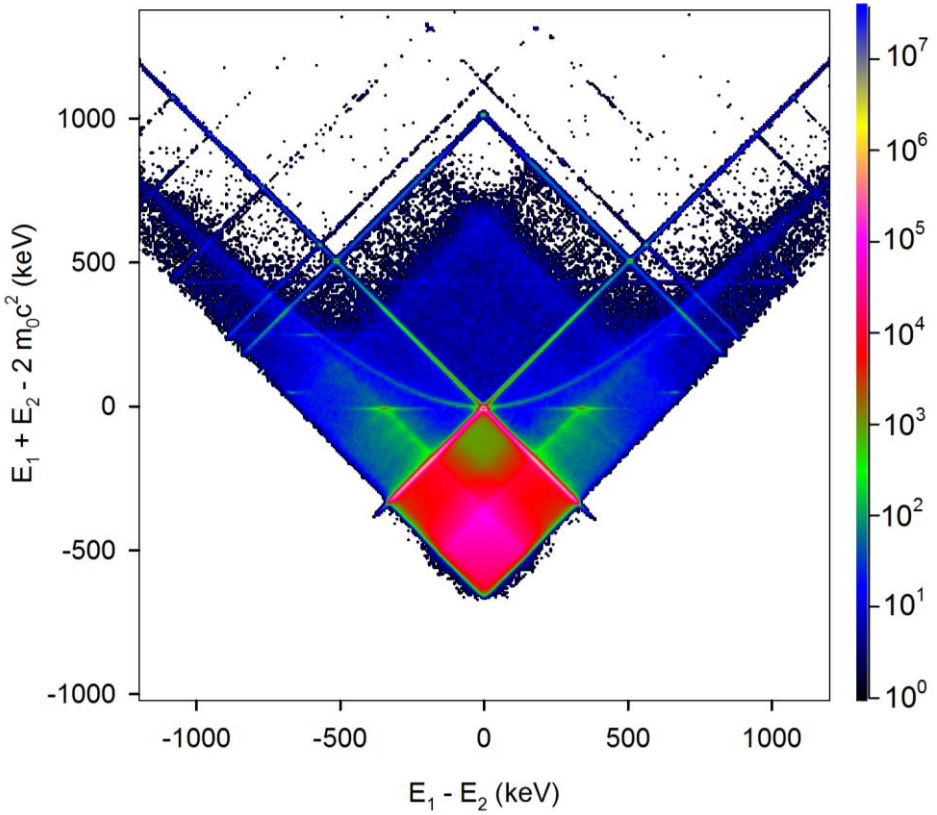

GiPS, W target, $T_+ \leq 16$ MeV

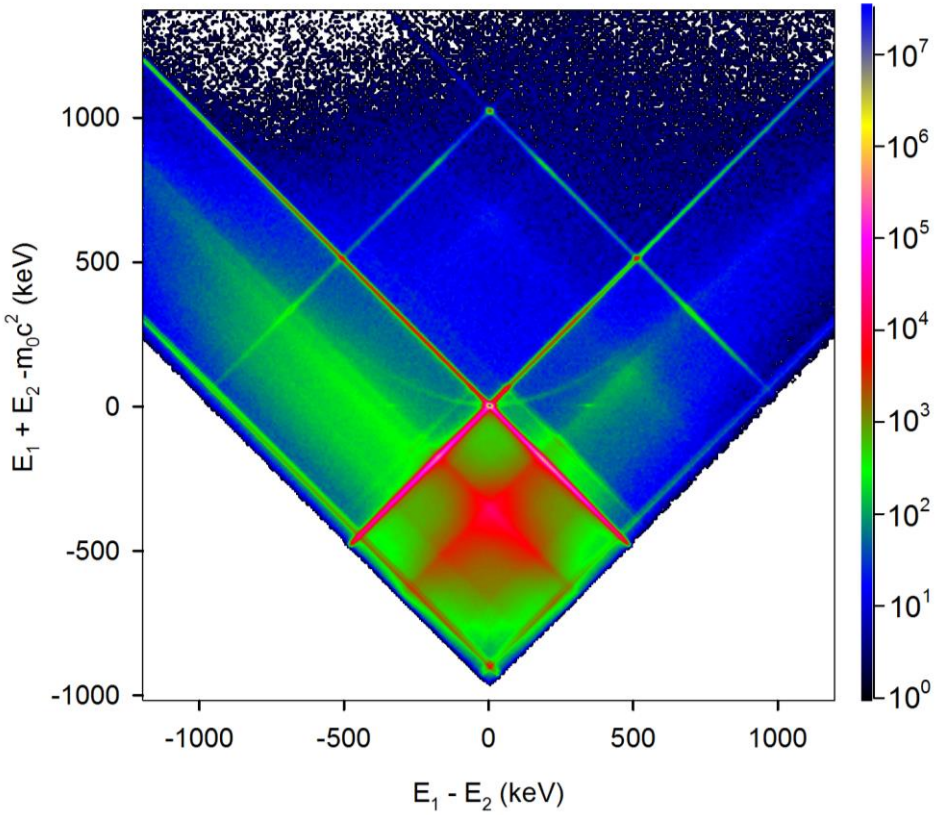

CDB spectra – fast positrons

- fast positrons, continuous energy spectrum
- larger distance for detectors from the target
- limited range of angles θ

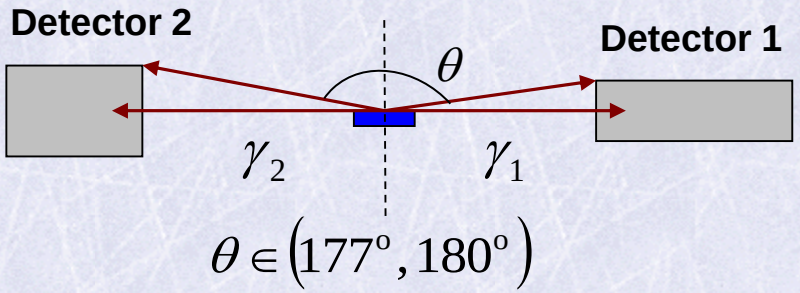

^{68}Ge/^{68}Ga, Mg target, $T_+ \leq 1897$ keV

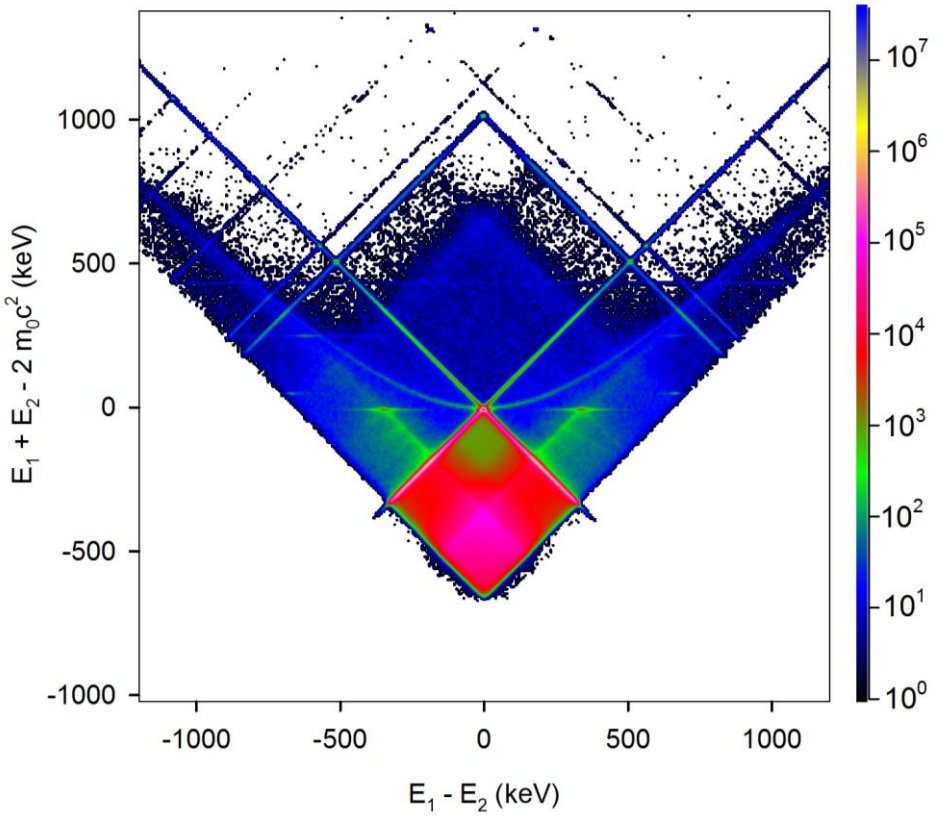

GiPS, W target, $T_+ \leq 16$ MeV

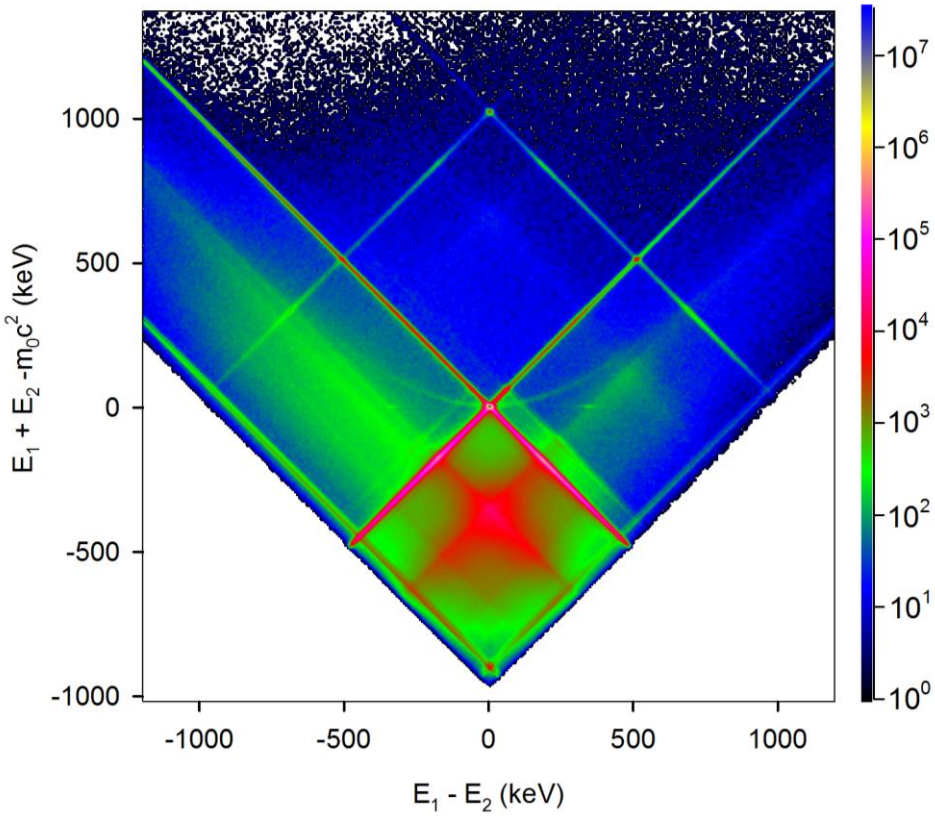

CDB spectra – fast positrons

- fast positrons, continuous energy spectrum

$$E_1 + E_2 - 2m_0c^2 = \sqrt{\left(E_1 - E_2\right)^2 + \left(m_0c^2\right)^2} - m_0c^2$$

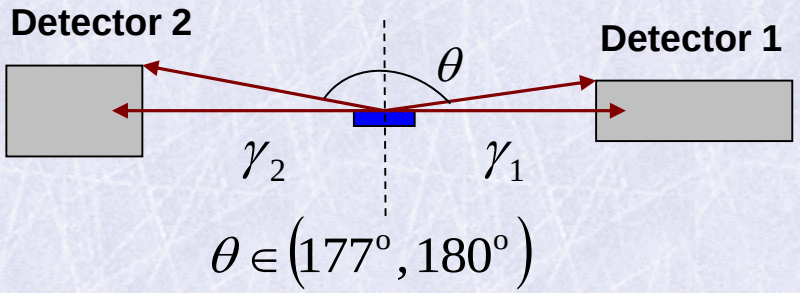

^{68}Ge/^{68}Ga, Mg target, $T_+ \leq 1897$ keV

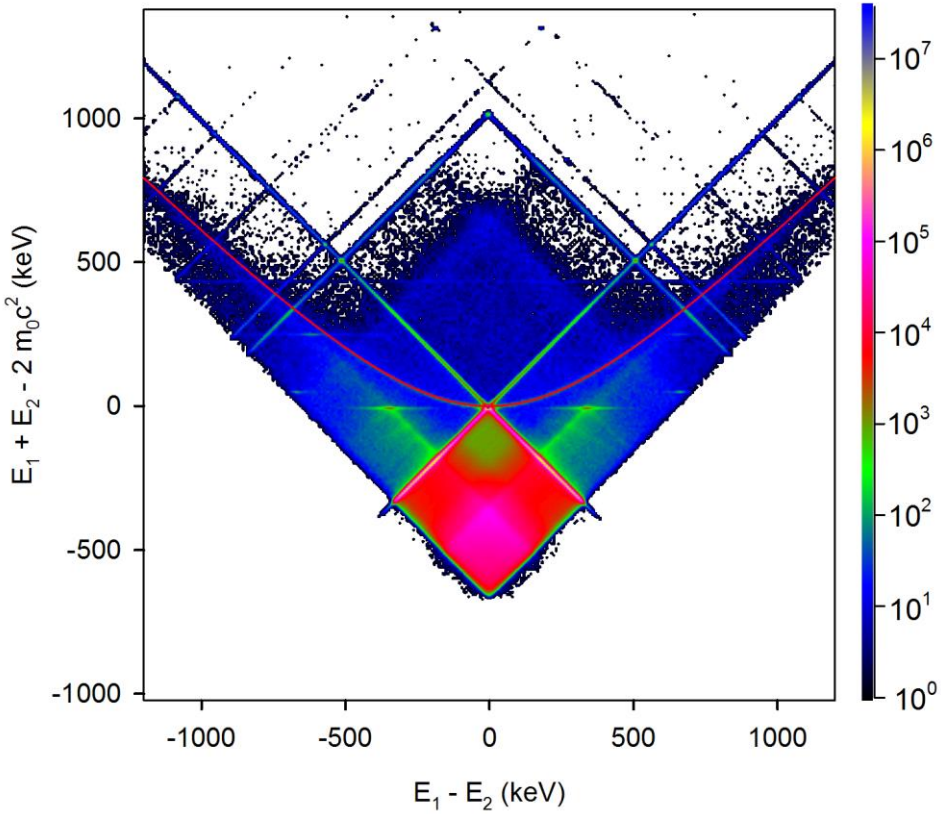

GiPS, W target, $T_+ \leq 16$ MeV

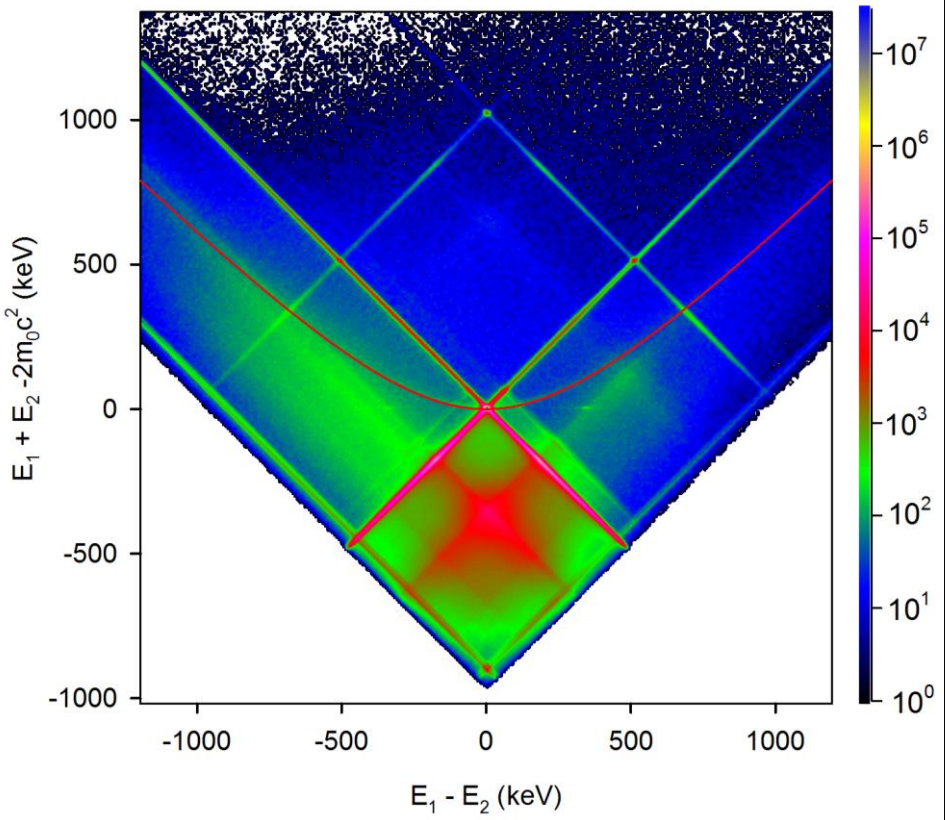

CDB spectra – fast positrons

- fast positrons, continuous energy spectrum
- higher kinematic cut-off
- GiPS: higher background due to scattering of bremsstrahlung radiation

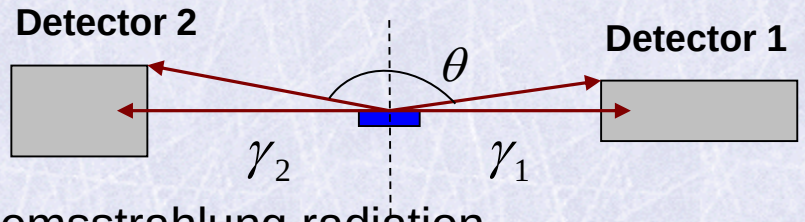

^{68}Ge/^{68}Ga, Mg target, $T_+ \leq 1897$ keV

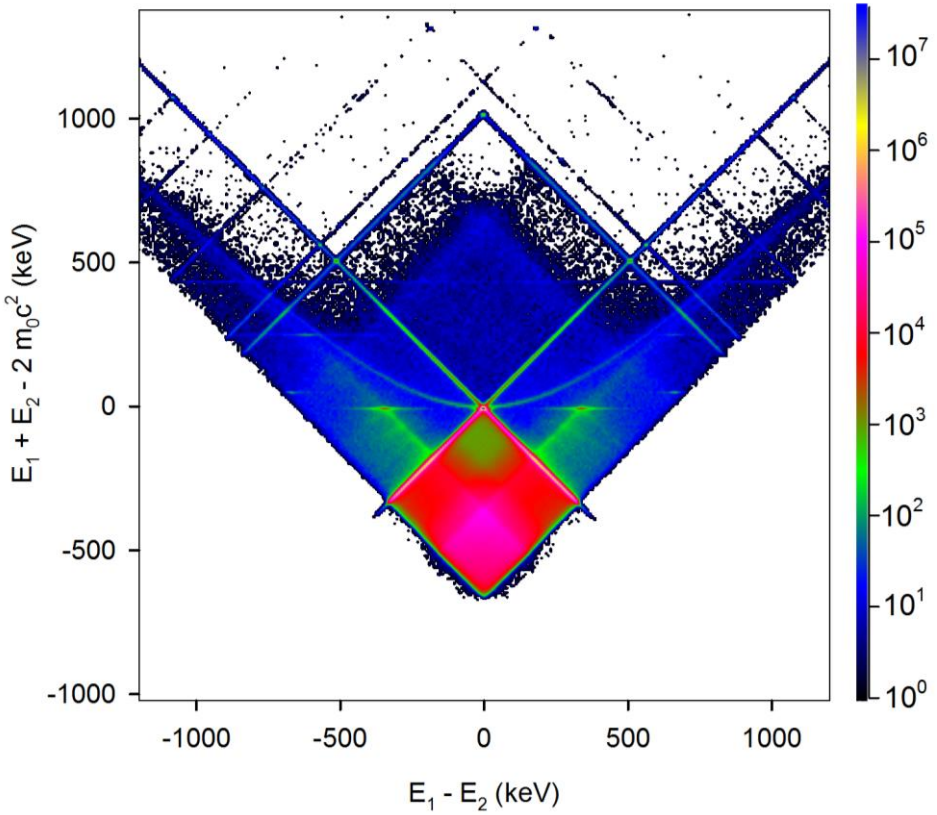

GiPS, W target, $T_+ \leq 16$ MeV

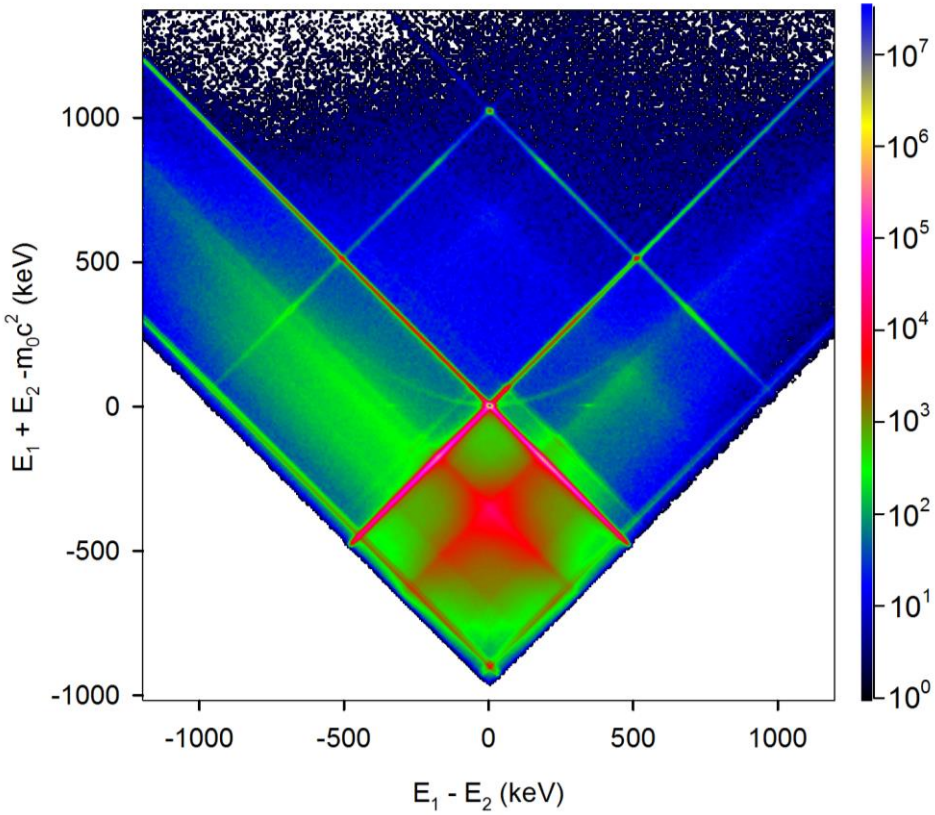

CDB spectra – fast positrons

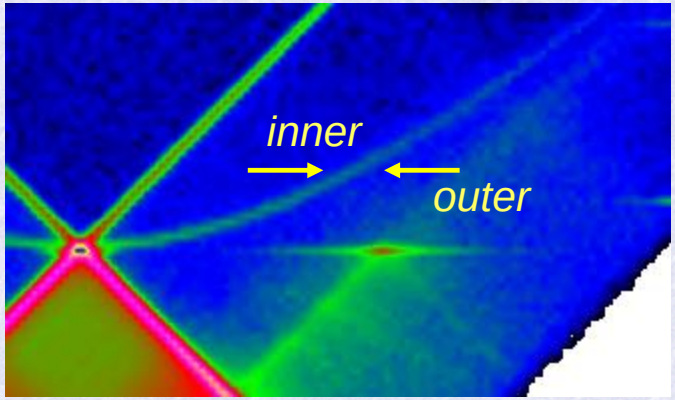

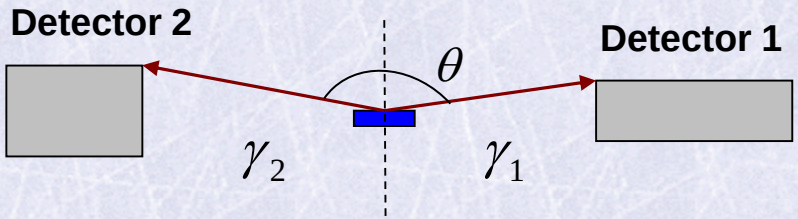

CDB spectra – fast positrons

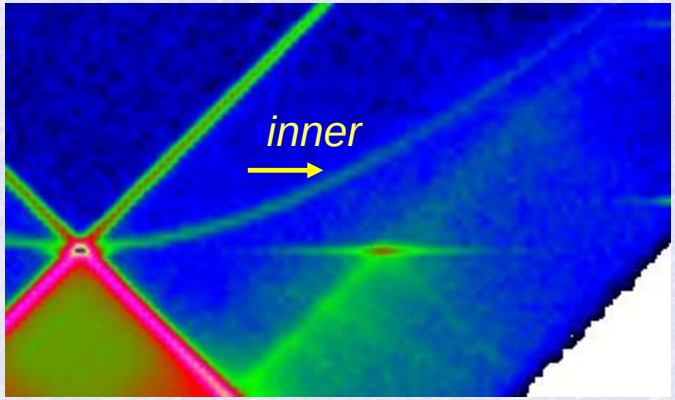

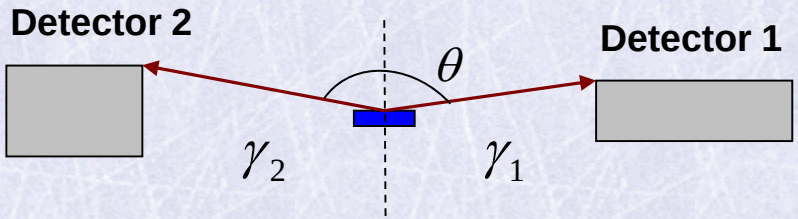

- ‘inner edge’ → finite size of detectors

CDB spectra – fast positrons

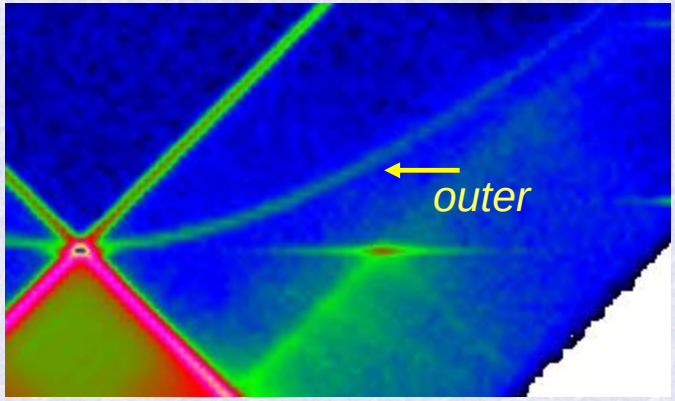

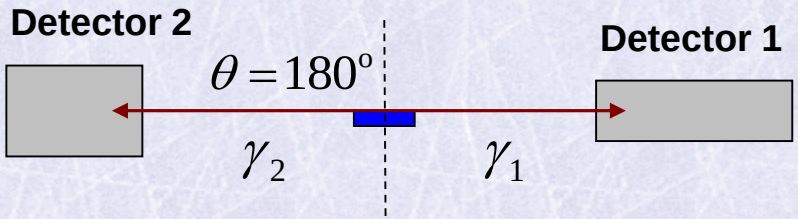

- ‘inner edge’ → finite size of detectors (instrumental effect)
- ‘outer edge’ → maximum Doppler shift (physical effect)
- annihilation in the rest: predominantly by low momentum valence e^-
- annihilation-in-flight: by all e^- with equal probability

↓

larger Doppler broadening ⟶ spectroscopy of core e^-

A.W. Hunt et al., Phys. Rev. Lett. 86, 5612 (2001)

CDB spectra – fast positrons

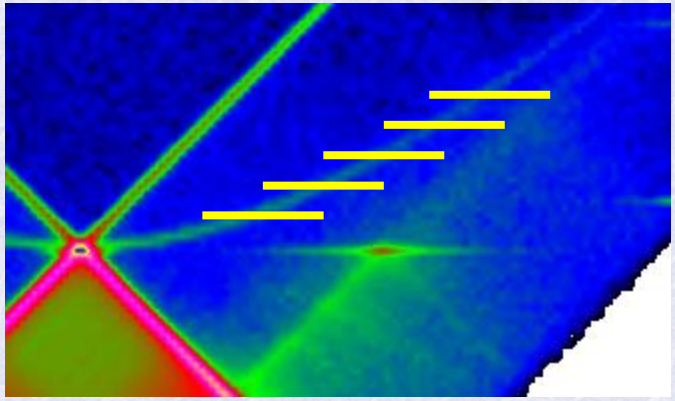

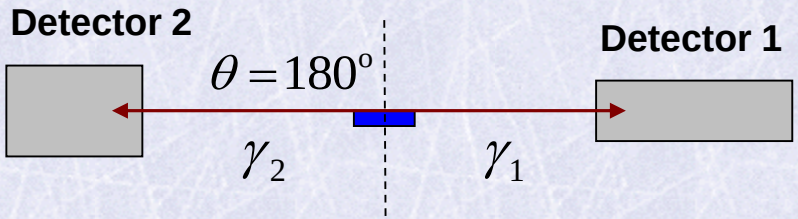

- ‘inner edge’ $\rightarrow$ finite size of detectors (instrumental effect)
- ‘outer edge’ $\rightarrow$ maximum Doppler shift (physical effect)
- Doppler broadening of the outer edge:
  - accumulated vertical stripes shifted along the TQAF curve

CDB spectra – fast positrons

- fast positron from $^{68}Ge/^{68}Ga$ source
- thick Mg target (thickness 10 mm)
- Doppler broadening of outer edge caused by annihilations with core e^-

TQAF (T_+ > 10 keV)

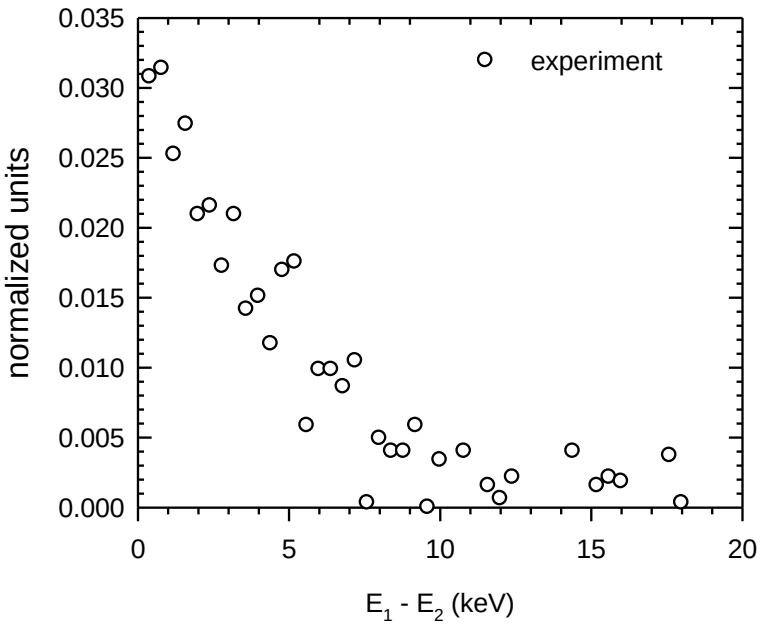

annihilation in the rest

CDB spectra – fast positrons

- fast positron from $^{68}Ge/^{68}Ga$ source
- thick Mg target (thickness 10 mm)
- Doppler broadening of outer edge caused by annihilations with core e^-

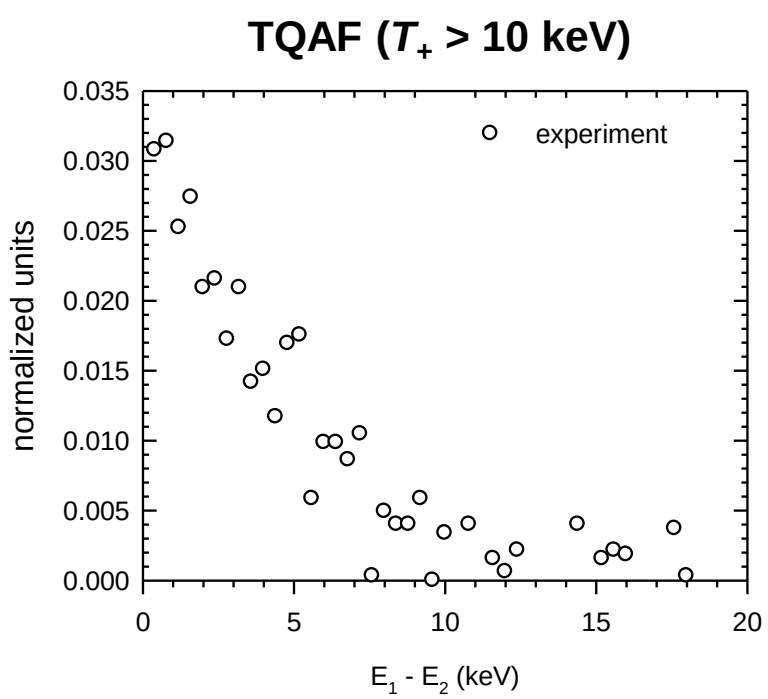

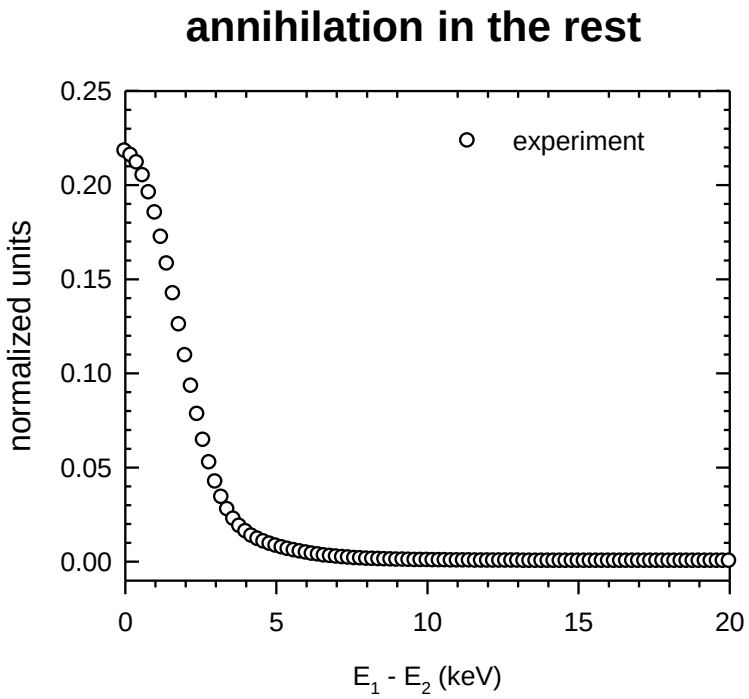

CDB spectra – fast positrons

- fast positron from $^{68}Ge/^{68}Ga$ source
- thick Mg target (thickness 10 mm)
- Doppler broadening of outer edge caused by annihilations with core e^-
- Mg: $\underbrace{1s^2\ 2s^2\ 2p^6}_{\text{core } e^-}\ 3s^2$

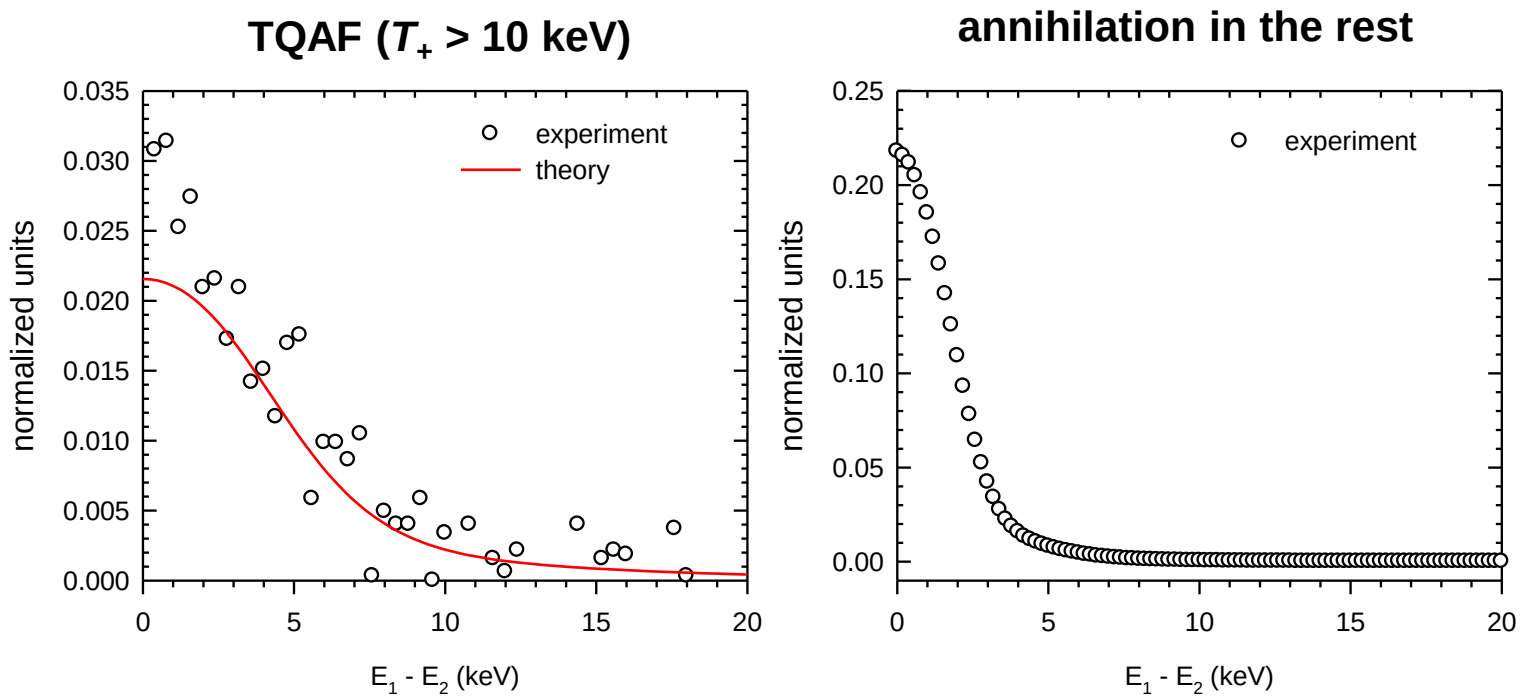

CDB spectra – fast positrons

- fast positron from $^{68}Ge/^{68}Ga$ source
- thick Mg target (thickness 10 mm)
- Doppler broadening of outer edge caused by annihilations with core e^-
- Mg: $\underbrace{1s^2\ 2s^2\ 2p^6}_{\text{core } e^-}\ 3s^2$

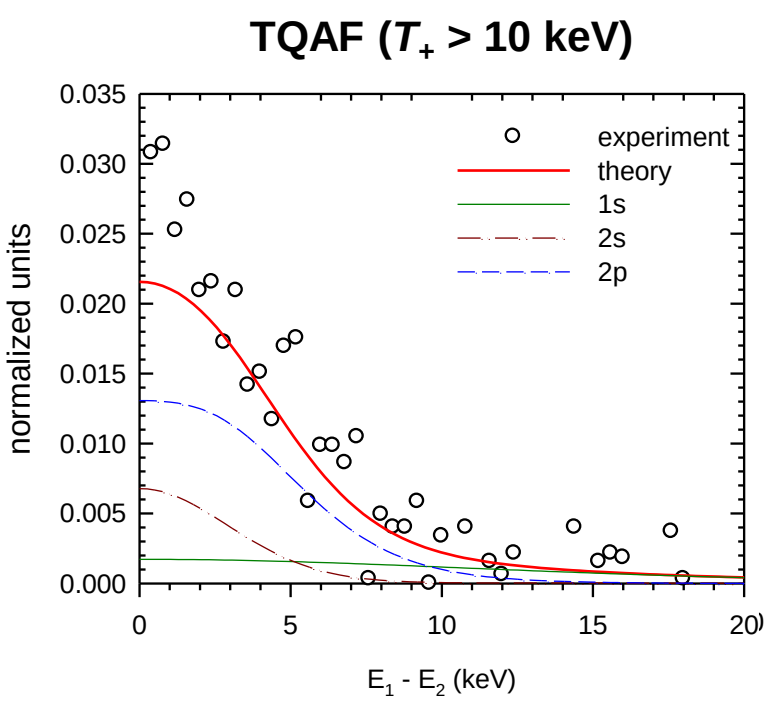

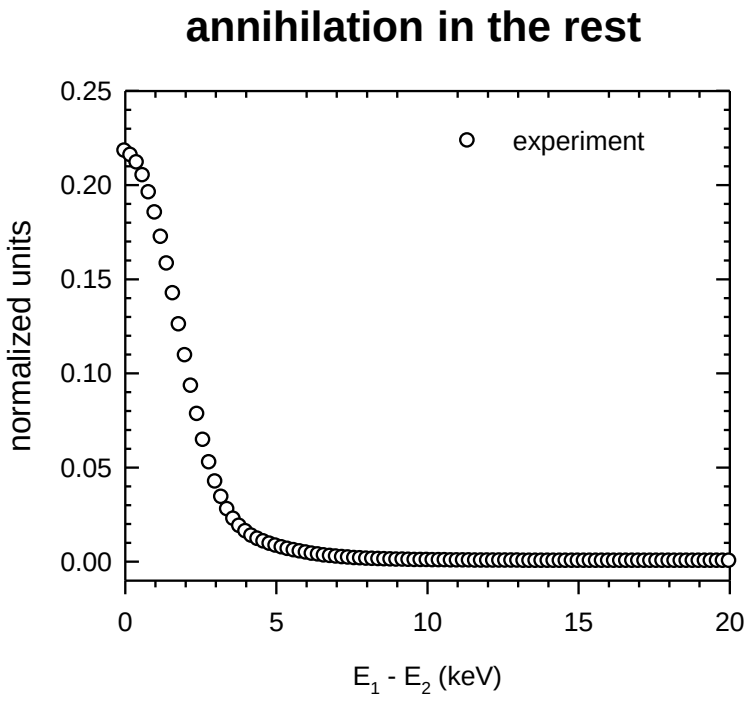

CDB spectra – fast positrons

- fast positron from $^{68}Ge/^{68}Ga$ source
- thick Mg target (thickness 10 mm)
- Doppler broadening of outer edge caused by annihilations with core e^-
- Mg: $\underbrace{1s^2\ 2s^2\ 2p^6}_{\text{core } e^-}\ 3s^2$

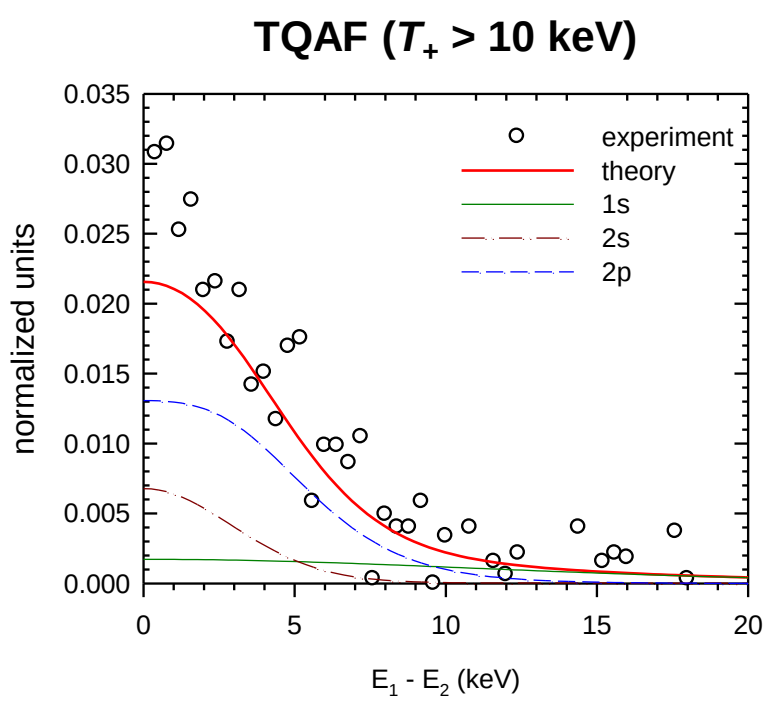

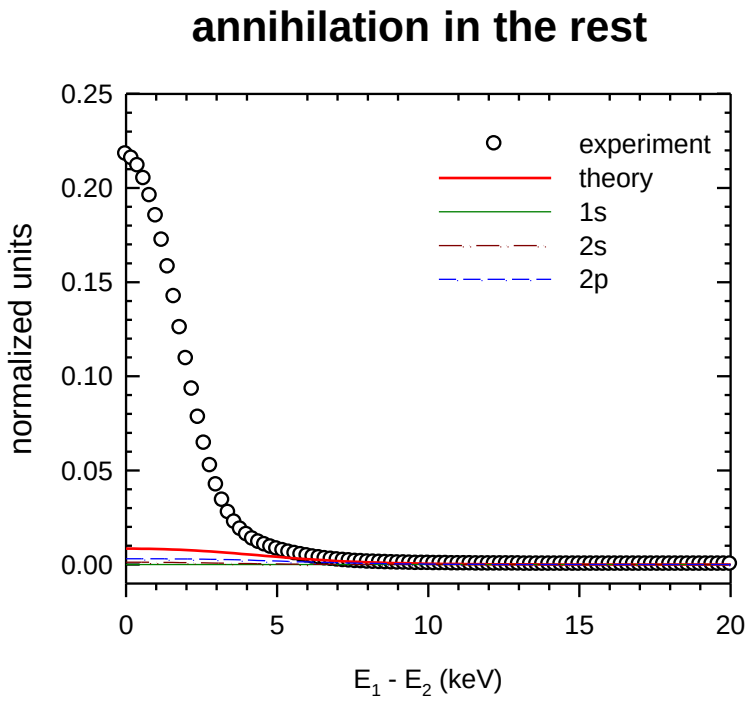

CDB spectra – fast positrons

- fast positron from $^{68}Ge/^{68}Ga$ source
- thick Mg target (thickness 10 mm)
- Doppler broadening of outer edge caused by annihilations with core e^-
- Mg: $\underbrace{1s^2\ 2s^2\ 2p^6}_{\text{core } e^-}\ 3s^2$

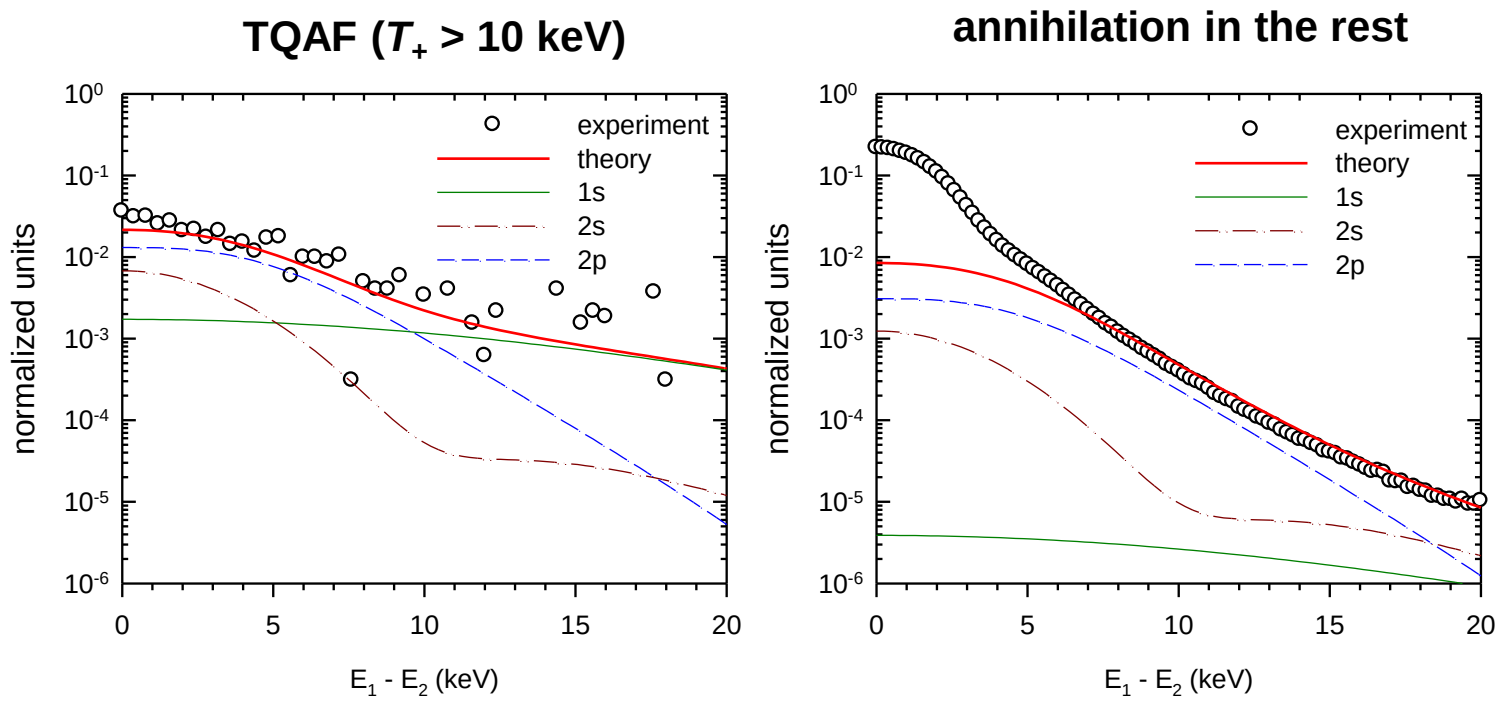

Conclusions

- A novel digital CDB spectrometer enables low background measurement of TQAF
- TQAF was investigated using positrons from various sources
  - monoenergetic positrons created in slow positron beam
  - fast positrons created by β^+ decay (^{68}Ge/^{68}Ga source)
  - fast positrons created by pair production from bremsstrahlung (GiPS source)
- Shape of TQAF contribution agrees well with theoretical prediction by QED
- TQAF profile provides information about positron slowing down
- CDB study of broadening of TQAF profile: a spectroscopy of core electrons
- a signature of o-Ps 3-γ annihilation observed in CDB spectra of slow e^+

Acknowledgements

This work was supported by The Czech Science Foundation (project P108/13/09436S). Availability of beam time at the ELBE, HZDR is gratefully acknowledged.